Journal of Medicinal Chemistry

pubs.acs.org/jmc

Article

Discovery of the S1P2 Antagonist GLPG2938 (1-[2-Ethoxy-6-(trifluoromethyl)-4-pyridyl]-3-[[5-methyl-6-[1-methyl-3-(trifluoromethyl)pyrazol-4-yl]pyridazin-3-yl]methyl]urea), a Preclinical Candidate for the Treatment of Idiopathic Pulmonary Fibrosis

Oscar Mammoliti,* Adeline Palisse,* Caroline Joannesse, Sandy El Bkassiny, Brigitte Allart, Alex Jaunet, Christel Menet, Beatrice Coornaert, Kathleen Sonck, Inge Duys, Philippe Clément-Lacroix, Line Oste, Monica Borgonovi, Emanuelle Wakselman, Thierry Christophe, Nicolas Houvenaghel, Mia Jans, Bertrand Heckmann, Laurent Sanière, and Reginald Brys

Cite This: *J. Med. Chem.* 2021, 64, 6037−6058

Read Online

ACCESS | Metrics & More | Article Recommendations | Supporting Information

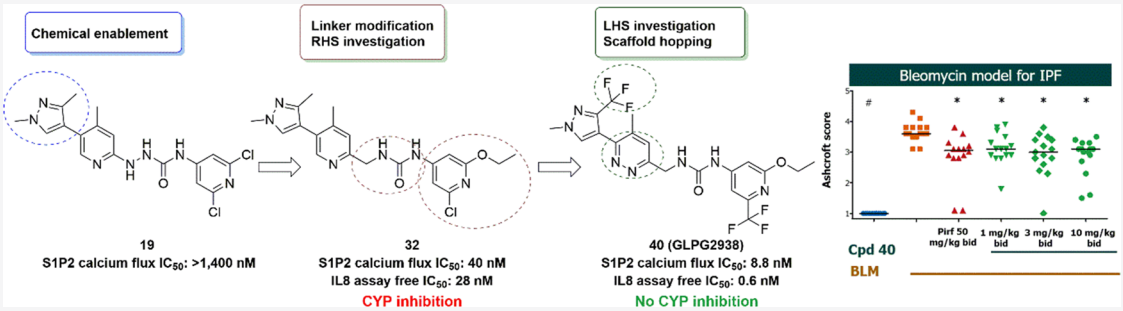

ABSTRACT: Mounting evidence from the literature suggests that blocking S1P2 receptor (S1PR2) signaling could be effective for the treatment of idiopathic pulmonary fibrosis (IPF). However, only a few antagonists have been so far disclosed. A chemical enablement strategy led to the discovery of a pyridine series with good antagonist activity. A pyridazine series with improved lipophilic efficiency and with no CYP inhibition liability was identified by scaffold hopping. Further optimization led to the discovery of **40** (GLPG2938), a compound with exquisite potency on a phenotypic IL8 release assay, good pharmacokinetics, and good activity in a bleomycin-induced model of pulmonary fibrosis.

INTRODUCTION

Sphingolipids are a class of membrane lipids. Apart from their structural role in membrane biology, they can also act as signaling messengers. Among them, lysophospholipid sphingosine-1-phosphate (S1P, Figure 1) plays a role in regulating a wide range of biological processes, including cell growth, cell survival, angiogenesis, and lymphocyte trafficking.[1] S1P is generated from sphingosine by phosphorylation of the C1 hydroxyl group. This process is mediated by sphingosine kinases (SPHK1 and SPHK2). The intracellular level of S1P is negatively regulated by S1P phosphatases (SGPP1 and SGPP2) and by sphingosine-1-phosphate lyase (SPL), which catalyzes the irreversible degradation of S1P to ethanolamine phosphate and 2-*trans* hexadecenal.[1b] The intracellular S1P is exported outside the cell by specific transporters, including SPNS2 (Sphingolipid Transporter 2). Extracellular S1P then signals through five G coupled protein receptors (GPCRs), S1P1, S1P2, S1P3, S1P4, and S1P5. S1P1, S1P2, and S1P3 are

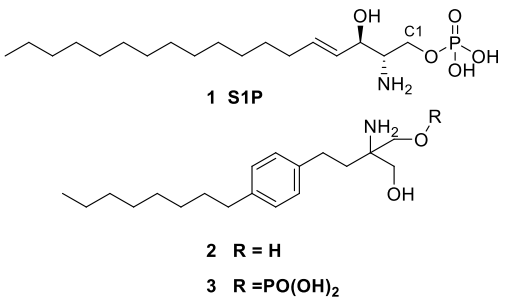

Figure 1. Structures of sphingosine-1-phosphate (S1P, **1**), FTY720 (**2**), and its active form, FTY720-P (**3**).

Received: January 24, 2021
Published: May 3, 2021

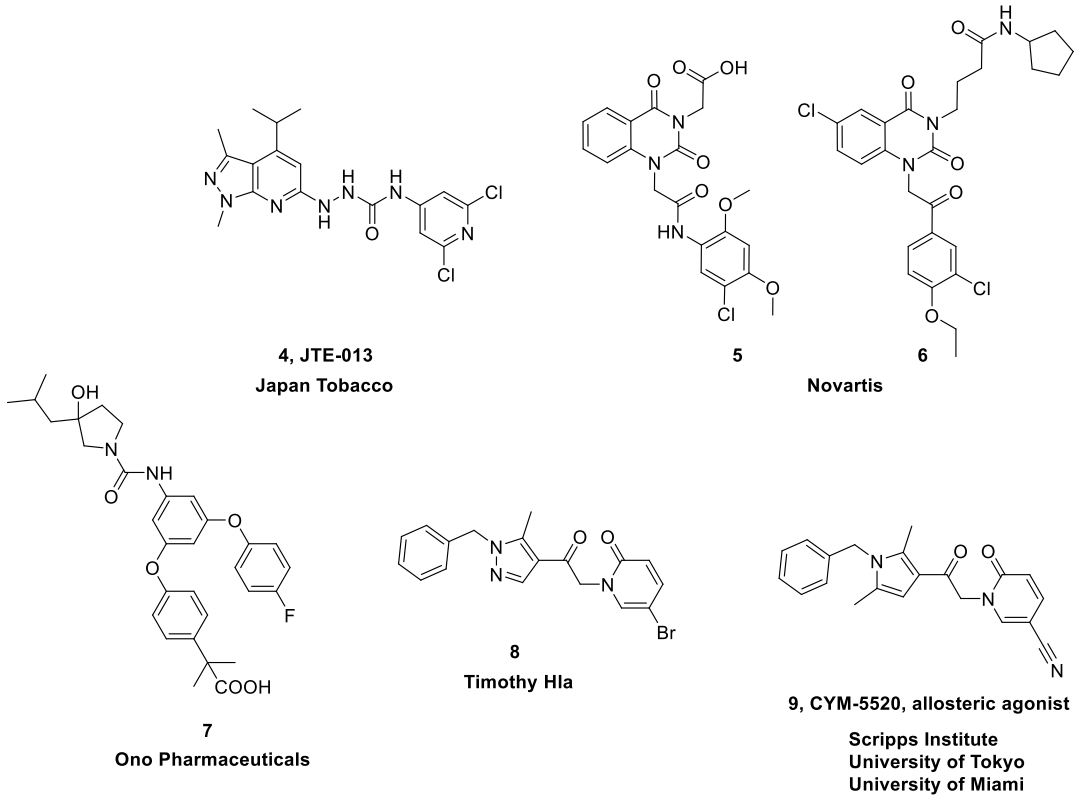

Figure 2. Examples of published S1P2 antagonists (**4**–**8**) and allosteric antagonist CYM-5520 (**9**).

widely expressed, while the expression of S1P4 and S1P5 is restricted to particular organs (lymphoid, hematopoietic, and pulmonary tissue for S1P4 and brain and spleen for S1P5).[2]

S1P1 activation promotes the lymphocytes egress from lymph nodes to sites of inflammation. In fact, modulation of the S1P1 receptor has demonstrated to be effective in multiple models of auto-immune diseases by depleting the circulating lymphocytes.[3] Moreover, Fingolimod (FTY720/Gilenya, compound **2**, Figure 1), a functional antagonist of S1P1, has been approved for relapsing multiple sclerosis.[4] FTY720 is a prodrug, which is activated *in vivo* by phosphorylation. The active form (FTY720-P, **3**) negatively modulates S1P1 by acting as an internalizing agonist.

On the other hand, FTY720 has also been associated to pro-fibrotic events in preclinical toxicological studies,[5] in animal models,[6] and in various *in vitro* settings.[7] In particular, Sobel *et al.* showed that FTY720-P caused a robust stimulation of extracellular matrix (ECM) deposition and induced fibrotic gene expression in normal human lung fibroblasts (NHLF).[8] These effects were attributed to S1P2 and S1P3 activation. This was in contrast with a previous report that showed that FTY720-P was not able to displace $S1^{33}P$ from membranes derived from S1P2 overexpressing CHO cells.[9] Sobel and colleagues, however, were able to show FTY720-P-mediated S1P2 receptor activation with impedance assays in different cell types. FTY720-P also induced an increased ECM synthesis in myofibroblasts; this effect was ascribed only to S1P2 modulation as expression levels of S1P3 were considerably low in those cells. Sobel *et al.* also showed that FTY720-P induced myofibroblast contraction, a phenomenon associated with fibrosis, in a S1P2-dependent manner.[10]

These reports came to join many other lines of evidence linking S1P2 activation to fibrotic diseases.[11] Among those, it has been reported that S1P2-deficient mice showed increased liver regeneration capacity and ameliorated fibrosis in liver injury models.[11g] S1P is increased in the bronchoalveolar lavage (BAL) fluid and in plasma of idiopathic pulmonary fibrosis (IPF) patients;[11h] it was also shown that S1P promotes endothelial to mesenchymal transition (EMT), a hallmark of fibrosis, in TGFβ-stimulated A549 cells by activation of S1P2 and S1P3.[11h] Very recently, it has been shown that S1P2-deficient mice have reduced inflammation and fibrosis markers in the bleomycin (BLM)-induced pulmonary fibrosis model.[12] Another account reported that genetic deletion of S1P2 resulted in attenuated lung fibrosis in the BLM mouse model. These effects were recapitulated by prophylactic administration of an undisclosed S1P2 antagonist.[13] All this evidence suggests that blocking S1P-mediated S1P2 signaling may be effective against fibrotic diseases.

It has been shown that in approximately half of the cases $S1P2^{-/-}$ mice develop cell lymphomas after 1.5–2 years of age.[14] This effect has been linked to the increase in germinal center (GC) B cells. Successive research, however, showed that, in humans, also another Gα13 coupled receptor, P2RY8, for which no orthologues have been identified in mice, promotes growth regulation and local confinement of GC B cells, suggesting a possible redundant role for S1P2.[15]

Despite the attractiveness of S1P2 as a target, only few documents describe the optimization of S1P2 antagonists[16] and there are no reports of clinical studies. This is in stark contrast with the number of S1P1 modulators that have entered clinical development.[17] Some representative S1P2 antagonists are highlighted in Figure 2. Notably, the first report of synthetic S1P2 antagonists[18] exemplifies the S1P2 antagonist JTE-013 (compound **4**, Figure 2), a compound that has been widely reported in the literature. Other

https://doi.org/10.1021/acs.jmedchem.1c00138
J. Med. Chem. 2021, 64, 6037–6058

noteworthy reports are from Novartis,[19] from Ono Pharmaceutical,[16,20] and, more recently, from Timothy Hla,[21] who describes S1P2 antagonists (e.g., compound **8**, Figure 2) whose structures are reminiscent of an allosteric agonist, CYM-5520 (compound **9**).[22]

Some of the antagonists so far described may have potential shortcomings. Novartis reported biological activity data only for a limited set of compounds, including compounds **5** and **6** (Figure 2). Compound **5** has a high TPSA (125.5) and a low clogD at pH 7.4 (−0.63, SimPlus)[23] combined with the presence of a carboxylic acid and three other carbonyls. The combination of these attributes could very well result in low permeability and, therefore, low oral absorption. On the other hand, compound **6** features highly lipophilic and flexible groups, which are potentially prone to oxidative metabolism. Ono Pharmaceutical has also been active in the field. Compound **7** constitutes an improvement from molecules previously reported, which were suffering from low bioavailability. However, despite good bioavailability in mice and dogs, bioavailability in monkeys was low (12%).[16c] Moreover, compound **7** possesses three benzene rings and the number of carboaromatic rings has been shown to correlate negatively with drug developability.[24] JTE-013 (compound **4**) features a hydrazine moiety, a functional group that has been associated with hepatotoxicity and drug-induced systemic lupus erythematosus.[25] JTE-013 has been extensively used as chemical probe in cellular assays. However, even though it has been proved to be a bona fide S1P2 antagonist, some reports call into question its selectivity and specificity.[26]

The biological evidence so far accumulated on the role of S1P2 in fibrosis prompted us to initiate a drug discovery campaign aiming at identifying S1P2 antagonists to validate this therapeutic hypothesis. Moreover, the limitations of existing S1P2 antagonists served also as a stimulus to provide improved chemical matter.

RESULTS AND DISCUSSION

To find new starting points, two consecutive HTS campaigns were conducted; however, they failed to identify progressable hits. We therefore decided to focus on a pyridine core to generate new chemical matter (Figure 3). Some S1P2 antagonists are based on fused bicyclic scaffolds, which are reminiscent of the 1*H*-pyrazolo[3,4-*b*]pyridine scaffold of the JTE-013 (e.g., compounds **10** and **11**, Figure 3).[27] In some cases, the 1*H*-pyrazolo[3,4-*b*]pyridine was redeployed, with different substituents.[27b,28] Synthesis and decoration of fused bicyclic scaffolds may entail long and laborious syntheses and also reduce the breadth of the explorable chemical space. For this reason, we opted for designs based on chemical enablement, which is "the efficient bond disconnection that facilitates the synthesis of libraries that probe multiple hypotheses".[29] To this end, the focus was placed on a new pyridine scaffold, which would allow to introduce a broad diversity of groups. For ease of synthesis, a methyl group was introduced instead of the recurring bulkier isopropyl group at the C4 position (Figure 3). This was also aiming at having a smaller pharmacophore. The newly introduced substituents may cause the scaffold to tilt in the binding pocket. In that case, the smaller methyl group could be a better fit for avoiding potential clashes with the protein.

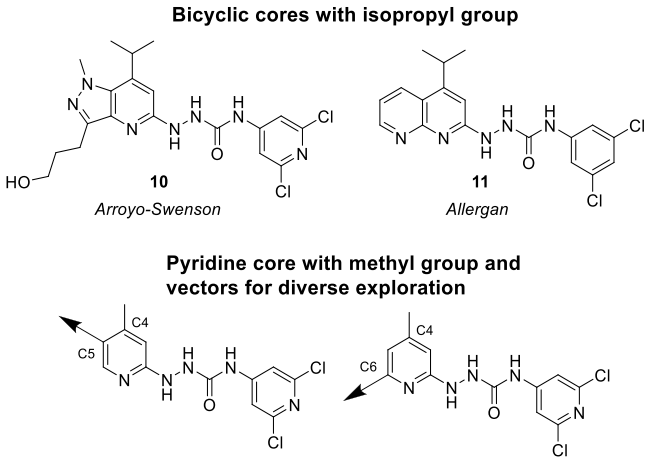

Figure 3. Chemical enablement to obtain S1P2 antagonists.

Two vectors were chosen for exploration, from the C5 and C6 position of the pyridine core, respectively. A structurally diverse set of groups was initially employed, with more than 40 compounds synthesized (a selection is presented in Table 1). To ensure the most effective receptor blockade, antagonists able to shut down S1P2 signaling across multiple pathways were sought.[30] To this end, potential antagonists were tested in a calcium flux assay (Gq involved) in CHO cells overexpressing the human S1P2 receptor, as well as in a GTPγS assay (mainly G_i involved), also based on the human S1P2 receptor. Small substituents, such as dimethylamino or CN, showed modest potency in both assays (compounds **12**−**15**). Aromatic groups, on the other hand, showed an improvement, with compound **19** displaying the best combination of potencies in the GTPγS and calcium flux assays, when tested in antagonist mode. None of the compounds showed any activity when tested in agonist mode (Table 1; this was also the case for all compounds reported in this manuscript; for this reason, it will not be mentioned further). Six-membered aromatic rings (such as **21**) were also active. However, the pyrazole motif was considered more attractive, in virtue of the reduced lipophilicity and size. The ethyl ester **16** showed submicromolar potency in the calcium flux assay. Ester groups, however, are potentially hydrolyzed very quickly by esterases, making them, most of the times, unsuitable for progression. For this reason, a few amide replacements were explored (compounds **22**−**24**). These derivatives, however, showed a marked drop in potency. Compounds **16**, **17**, and **19** were able to compete with radiolabeled S1P in membranes derived from stable cell lines overexpressing the human S1P2 receptor. This indicated that these compounds were most probably orthosteric antagonists. Again, compound **19** was the most potent and, in virtue of this, it was selected for further optimization.

Finding a replacement for the hydrazine urea was the next focus of the optimization. Some examples from the literature showed that it was possible to replace the hydrazine linker on fused bicyclic scaffolds.[27a] It could not be anticipated, however, if those replacements would have been compatible with the pyridine scaffold. Designs were guided by the idea of keeping a hydrogen bond donor and a hydrogen bond acceptor at the same distance from the core as in the hydrazine-based molecules showed in Table 1. The hydrogen bond donor was connected to the core by a benzylic CH_2 instead of an NH spacer (Table 2). Compounds were also profiled for liver microsomal stability. Scaled clearance values, corrected for microsomal binding (fu, mic), were used (Clint, u, see eqs

https://doi.org/10.1021/acs.jmedchem.1c00138
J. Med. Chem. 2021, 64, 6037−6058

Table 1. Initial Exploration of the Pyridine Core: LHS Modifications

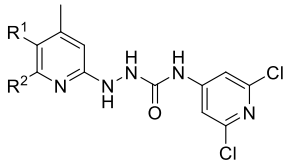

Nr	R^1	R^2	S1P2 calcium flux anta[a] *(ago)*[b] IC_{50} (μM)[c]	S1P2 GTPγS IC_{50} (μM)[c]	S1P2 competition binding assay IC_{50} (μM)[c]
12			3.6[d] *(>23)*[d]	5.3[d]	NT
13			6.0[d] *(>23)*[d]	7.0	NT
14			>6.6[d] *(>23)*[d]	NT	NT
15			>6.6[d] *(>23)*[d]	31[d]	NT
16			0.76 *(>23)*	2.1[d]	0.30[d]
17			2.6[d] *(>23)*[d]	3.4	1.2[d]
18			4.0 *(>23)*	9.3[d]	NT
19			>1.4[e] *(>23)*	0.8	0.19[d]
20			>2.1[e] *(>23)*	3.1	NT
21			1.3[d] *(>23)*[d]	6.2[d]	NT
22			>19[d] *(>23)*[d]	NT	NT
23			4.5[d] *(>23)*[d]	NT	NT
24			>20[d] *(>23)*[d]	NT	NT

[a]Assay run in antagonist mode. [b]Assay run in agonist mode. [c]Experiments aiming at determining the IC_{50} values were performed at least twice, unless otherwise stated. When multiple experiments were performed, the geometrical mean is provided. [d]n = 1. [e]IC_{50} for each run (n = 5) in Supporting Information, Table S10. NT = not tested.

3−5, Experimental Section). The benzimidazole-based compounds **25** and **26** showed good potency, but they also showed high *in vitro* clearance in mouse liver microsomes (MLMs). Indoles **27** and **28** possessed good potency, but, also in this case, the *in vitro* clearance was too high (Clint, u > 34 L/h/kg). Amides **29** and **30** resulted in total loss of activity. Urea **31**, on the other hand, displayed submicromolar potency in both GTPγS and calcium flux assays. A quick exploration of the aromatic right-hand side led to urea **32**, which had improved potency in comparison with **31**. Compound **32** showed also a marked improved LipE[31] (obtained from the calcium flux assay and clogD). The right-hand side pyridine conferred to **31** a much greater microsomal stability comparing with the phenyl ring of matched pair **33** (>10x), highlighting the importance of this group for metabolic stability. The compounds were also profiled in a phenotypic assay based on S1P-stimulated IL8 production in human lung fibroblasts (HFL1). Elevated levels of IL8, a neutrophilic chemoattractant, have been linked to IPF[32] and S1P has been shown to stimulate IL8 secretion by signaling through S1P2.[33] The majority of the compounds in Table 2 presented IC_{50} values in the IL8 assay in line with the GTPγS assay. Compounds **32** and **33** showed the highest shift (5x).

To ameliorate clearance and further improve potency, a broader exploration of the C5 position of the pyridine was undertaken (Figure 4). To this end, a chemical enablement strategy based on a urea protecting group was implemented (Scheme 5). The protecting group allowed us to perform certain reactions, such as Buchwald and Ullmann couplings, in a convergent fashion. The 2-ethoxy-6-(trifluoromethyl)pyridin-4-amine group was selected for the right-hand side. This group conferred a level of potency similar to the 2-chloro-6-ethoxypyridin-4-amine group (cfr **34** and **98**, Supporting Information), but it had also the advantage to be unreactive in cross-coupling conditions, while the 2-chloro-6-ethoxypyridin-4-amine could potentially react on the C2 position. Following this and other less convergent approaches, some of them described above, more than 60 analogs were prepared to broadly investigate the C5 position (the full SAR is shown in Table S4, Supporting Information). Essentially three chemotypes were explored: CC-linked (hetero)aryl groups, (hetero)alkyl/(hetero)aryl secondary amines, and (hetero)alkyl tertiary amines (green, orange, and blue, respectively, in Figure 4). The CC-linked (hetero)aryls and the secondary amines showed high potency in both calcium flux and GTPγS assays, while the tertiary amines were in general less potent, especially in the GTPγS assay. Some of the compounds were profiled in the IL8 phenotypic assay and in the microsomal stability assay. Only few compounds showed a good balance between potency and clearance. The best compound in this aspect for each chemotype is shown in Table 3.

The CF_3 group in **34** was an improvement in comparison with the methyl group of matched pair **32**, especially in the IL8 phenotypic assay (7x improvement, Table 3). To measure the phenotypic activity in a more physiological setting, compounds **32** and **34** were tested in the presence of 2% human serum albumin (HSA, equivalent to approximately 40% serum). Serum could not be used as it contains S1P. The presence of HSA could also offset potential binding to plastics and medium for more lipophilic compounds, leading to a better estimate of the relevant free IC_{50}. The free IC_{50} values were obtained estimating the fraction unbound in the medium (fu, medium) from the human plasma protein binding (hPPB) according to eqs 1 and 2 in the Experimental Section.[34] For a set of compounds, the binding to the assay medium containing HSA was directly measured and it was in agreement with the binding calculated from PPB values. For **32** and **34**, the absolute IC_{50} values in the presence of HSA were 3039 and 572 nM, while the free IC_{50} values were 28 and 1.4 nM, respectively. The improvement for **34** was thus greater than the 1 log unit increase in lipophilicity.

Also, compounds **35** and **36** showed good potency (with **36** being somewhat weaker in the GTPγS assay) and improved clearance. However, none of them was superior to **34**. The secondary amines, like **35**, showed a similar profile to CC-linked derivatives, with no apparent advantage to compensate for the extra H bond donor. Therefore, they were not investigated further. For the tertiary amines, like **36**, the data

https://doi.org/10.1021/acs.jmedchem.1c00138
J. Med. Chem. 2021, 64, 6037−6058

Table 2. Linker Optimization in the Pyridine Scaffold

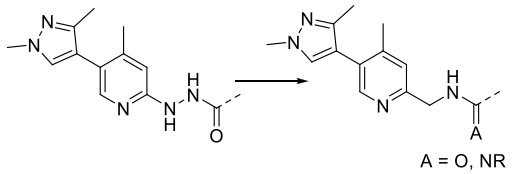

Nr	Structure	clogD	S1P2 calcium flux[a] IC_{50} (μM)[b] (**LipE**)	S1P2 GTPγS IC_{50} (μM)[b]	IL8 IC_{50} (μM)[b]	Clint, u[d] mouse (L/h/kg)
25	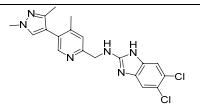	4.2	0.099 (**2.8**)	0.43[c]	0.21	155[e]
26	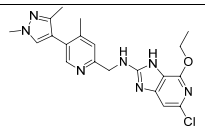	3.3	0.033[c] (**4.2**)	2.25[c]	1.30[c]	82
27	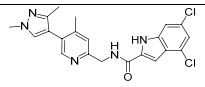	4.0	0.11 (**3.0**)	0.61[c]	>1.11[f]	<47[e]
28	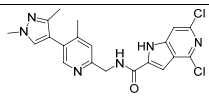	3.3	0.89[c] (**2.8**)	1.3[c]	NT	38
29	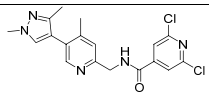	3.0	>19[c] (**<1.7**)	>100[c]	NT	5.1
30	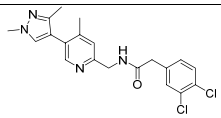	3.7	>19[c] (**<1.0**)	NT	NT	226
31	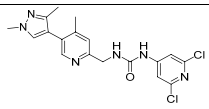	3.0	0.30 (**3.5**)	0.77[c]	2.05[c]	12
32	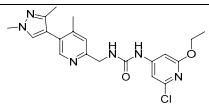	2.6	0.040 (**4.7**)	0.032[c]	0.15	42
33	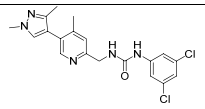	3.6	0.16[c] (**3.2**)	0.30[c]	0.16[c]	159

[a]Antagonist mode. [b]Experiments aiming at determining the IC_{50} values were performed at least twice, unless otherwise stated. When multiple experiments were performed, the geometrical mean is provided. [c]$n = 1$. [d]Fraction unbound in microsomes (fu, mic) experimentally determined, unless otherwise stated. [e]Fu, mic calculated. [f]Precipitation at high dose. NT = not tested.

indicated that it could be more challenging to obtain a good balance between potency and clearance (Figure 4). For this reason, their progression was also put on hold.

The new lead **34** displayed strong CYP inhibition (recombinant 2C19, 2C9, and 3A4, 100%, 83%, and 83% inhibition at 10 μM, respectively, Table S5, Supporting Information). CYP inhibition was a general feature of the pyridine series. To remove this liability, and to improve clearance, a scaffold hopping strategy privileging more polar cores was envisaged. A pyridazine-based scaffold was selected and synthesized. The benefits of the CH to N switch have already been reviewed elsewhere.[35] Compound **37** (Table 4) retained good potency with lower lipophilicity, thus resulting in an improved LipE (4.4 vs 5.0). CYP inhibition was mitigated (recombinant 2C19, 2C9, and 3A4, 61%, 58%, and 23% inhibition at 10 μM, respectively, Table S5, Supporting Information). Clearance was improved, especially in human liver microsomes. A broader analysis of matched pairs between the pyridine and the pyridazine scaffolds clearly showed the latter to be an improvement as all matched pairs had better LipE (Figure 5).

The exploration of the right-hand side was the next focus of the optimization. At first, pyridine-4-amines with two substituents (C2 and C6 positions) were evaluated (**37**–**45**,

https://doi.org/10.1021/acs.jmedchem.1c00138
J. Med. Chem. 2021, 64, 6037−6058

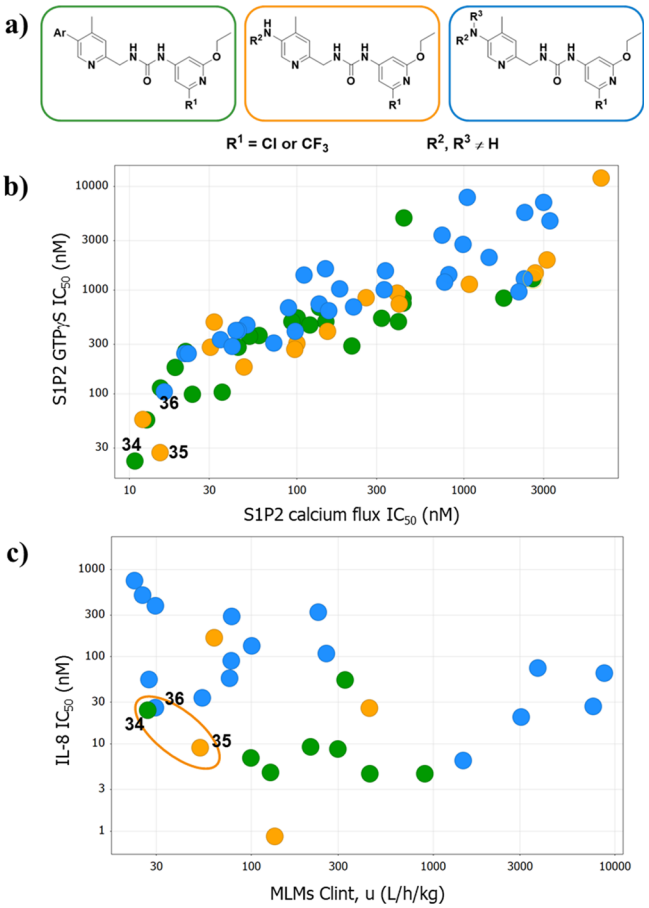

Figure 4. Broad exploration of pyridine's C5 position by a chemical enablement strategy. (a) Representation of chemotypes. (b) Potency in calcium flux assay vs potency in GTPγS assay. (c) Clearance unbound in mouse liver microsomes vs potency in IL8 assay.

Table 4). In the presence of the ethoxy group, electron-withdrawing substituents showed good potencies (Cl, CN, and CF_3 in **37**, **39**, and **40**, respectively). **40** was exquisitely potent in the IL8 assay (free IC_{50}: 0.60 nM). Replacement of the electron-withdrawing groups by a methyl group in **41** resulted in a considerable loss of potency (5−10x) across all assays. The compounds from this set showed in general good microsomal stability, especially in humans. Replacement of the ethyl group in **37** by a CH_2CHF_2 group was tolerated (**38**). On the other hand, more polar groups were poorly tolerated (**42** and **45**) or lost all activity (**43** and **44**).

In a second set of compounds (**46**−**51**), the C3 position of the right-hand side pyridine-4-amine was investigated. This position was selected in reason of the ortho directing properties of the alkoxy groups, which allowed for a regioselective bromination at the C3 position for further derivatization (Scheme S4, Supporting Information). Methyl substitution in compounds **46** and **47** resulted in similar potency in the calcium flux and GTPγS assays comparing with matched pairs **37** and **39**. This change resulted, however, in a marked increase in potency in the IL8 phenotypic assay (about 10x for both compounds). When this change was applied to **41**, an increase in potency of about 10x in all assays was obtained (compound **48**). This "magic methyl" effect[36] was also accompanied by retention of good metabolic stability (human) and improved LipE. A chlorine atom had a very similar effect for compound **50**. Replacement with CN resulted in total loss of activity (compound **51**). Other groups were investigated, but, in general, they resulted to be worse than the methyl group and chlorine atom.[37]

The exploration of the right-hand side resulted in molecules with very good potency and microsomal stability. Compounds **37**, **40**, and **48** were therefore selected for pharmacokinetic studies in preclinical species. The potent compound **47** was excluded because it showed tolerability issues after single dose administration (both iv and po) in mice. Compound **37** showed low to moderate half-life across species and low bioavailability in general (Table 5). Therefore, it was not progressed further, also considering its low solubility. Compound **40**, on the other hand, showed good pharmacokinetics, with long half-life, low clearance, and good bioavailability in all species, especially in dogs. Plasma protein binding was quite high; from the PK data, however, a free concentration covering the IL8 IC_{50} was attainable. Although solubility was low both in FaSSGF and FaSSIF media, this did not forbid to obtain good bioavailability with simple formulations, at least at low doses in mice and dogs. Compound **48**, on the other hand, showed shorter half-life and higher clearance in all species comparing with **40**, while having a markedly increased solubility in the FaSSGF medium (>200x). This improvement resulted most probably from the basicity of the pyridine group (measured pKa: 4.32), which allowed the compound to have high solubility in the FaSSGF medium (pH = 1.6). The pKa of **40** could not be measured,

Table 3. Broad Investigation of Pyridine's C5 Position: Best Compounds per Chemotype

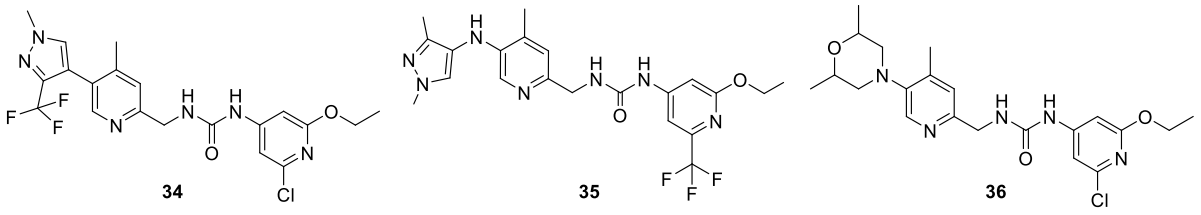

Cpd	clogD	S1P2 calcium flux[a] IC_{50} (nM)[b] (**LipE**)	S1P2 GTPγS IC_{50} (nM)[b]	IL8 IC_{50} (nM)[b]	Clint, u[d] mouse/human (L/h/kg)
34	3.6	11 (**4.4**)	22[c]	23	27/9.0
35	3.1	12[c] (**4.8**)	55	7.4	52/16
36	3.6	16 (**4.2**)	105	23	30/7.5

[a]Antagonist mode. [b]Experiments aiming at determining the IC_{50} values were performed at least twice, unless otherwise stated. When multiple experiments were performed, the geometrical mean is provided. [c]n = 1. [d]Fraction unbound in microsomes (fu, mic) experimentally determined, unless otherwise stated. NT = not tested.

https://doi.org/10.1021/acs.jmedchem.1c00138
J. Med. Chem. 2021, 64, 6037−6058

Table 4. SAR of Right-Hand Side Groups in the Pyridazine-Based Series

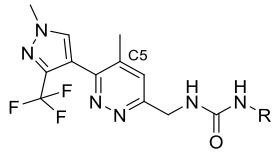

Cpd	R	clogD	S1P2 calcium flux[a] IC_{50} (nM)[b] (**LipE**)	S1P2 GTPγS IC_{50} (nM)[b]	IL8 IC_{50} (nM)[b]	IL8 IC_{50} 2% HSA IC_{50} (**free**) (nM)[b]	Clint, u mouse / human (L/h/kg)
37	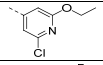	3.0	7.7 (**5.0**)	20	2.8	45 (**1.0**)	<23 / <2.6
38	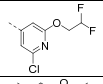	3.0	7.2 (**5.1**)	36	4.2	71 (**1.3**)	<10 / <3.0
39		2.5	11 (**5.5**)	35	11	67 (**3.0**)	<6.3 / <1.7
40	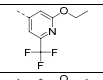	3.2	8.8 (**4.9**)	29	3.8	87 (**0.60**)	8.4 / <2.3
41	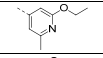	2.9	54 (**4.4**)	242[c]	37	194 (**15**)	<3.5 / <0.9
42	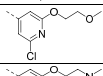	2.9	412 (**3.5**)	640[c]	1650[c]	3220[c] (**NT**)	19 / <1.4
43	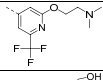	2.7	2139[c] (**3.0**)	>10000[c]	NT	NT (**NT**)	<5.4 / 1.4
44	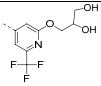	2.2	> 6610[c] (**<3.0**)	>11000[c]	1540[c]	>10000[c] (**NT**)	<4.6 / 1.9
45	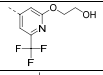	2.5	348[c] (**4.0**)	704	236	810 (**87**)	6.1 / <1.4
46	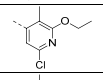	3.3	8.8 (**4.8**)	15	0.42	32 (**0.16**)	<32 / <7.6
47		2.6	7.1 (**5.5**)	24	0.59	17 (**0.19**)	<9.8 / <2.1
48	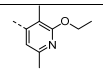	3.1	4.5 (**5.2**)	16	3.1	49 (**1.3**)	17 / 2.2
49	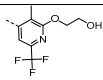	2.7	84[c] (**4.4**)	160	47	256 (**5.4**)	<5.3 / NT
50	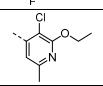	3.2	8.7 (**4.9**)	26	2.4	49 (**0.55**)	15 / <1.5
51	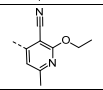	2.6	>20000[c] (**<2.1**)	>20000[c]	2740[c]	>30000[c] (**NT**)	136 / <1.2

[a]Antagonist mode. [b]Experiments aiming at determining the IC_{50} values were performed at least twice, unless otherwise stated. When multiple experiments were performed, the geometrical mean is provided. [c]n = 1. [d]Fraction unbound in microsomes (fu, mic) experimentally determined, unless otherwise stated. NT = not tested.

indicating lack of protonation even at low pH values. Solubility, even when limited to low pH values, was deemed important in order to achieve dose-proportional exposure in toxicology studies, when usually high doses are administered.

Other compounds were designed and synthesized to improve solubility, specifically by replacing the methyl group at the N1 position of the pyrazole or the methyl at the C5 position of the pyridazine core with more polar groups.[37] None of these compounds, however, possessed a balanced profile in terms of potency, metabolic stability, and solubility in order to be progressed further.

Compound **40** confirmed to be active against S1P2 in the radioligand-based binding assay as well as in an arrestin-based assay. It was also potent against the murine S1P2 receptor (mS1P2, arrestin assay, Table S1, Supporting Information). In terms of selectivity, **40** did not have any meaningful activity against any of the other S1P receptors (Table S1, Supporting Information). When profiled against a broad panel of receptors, transporters, and enzymes (Cerep Diversity Panel, compound tested at 10 μM), only a few targets were picked up with inhibition, binding, or activation >50%. Follow up dose responses on eight targets showed IC_{50} values to be only in the micromolar range for all these targets (Table S3, Supporting Information). Compound **48** was also active against mS1P2 and showed complete selectivity against the other S1P receptors (Table S2, Supporting Information). No meaningful inhibition, binding, or activation was picked up in the Cerep Diversity Panel. Both **40** and **48** showed no meaningful inhibition against a panel of 154 kinases when tested in a single dose at 1 μM.

Compound **40** was tested in a cell contraction assay with human pulmonary fibroblasts (HPFs). Fibroblast contraction is a phenomenon observed during wound healing as well as in many fibrotic disorders.[10] In the cell contraction assay, myofibroblasts that have been pre-treated with TGF-β for 4 days are suspended in a collagen gel lattice mixture. Stress build-up continues for another 3 days. Upon release of the gels from the well, the gel lattice will start to shrink due to the myofibroblast contraction, which can be further stimulated by S1P addition, resulting in a reduced surface area. As it could be seen in Figure 6, compound **40** significantly prevented the S1P-mediated contraction at all tested concentrations.

From the data presented above, compounds **40** and **48** emerged as potent and selective S1P2 antagonists with good ADMET and PK. This and their confirmed potency against the murine S1P2 receptor made them suitable candidates for the bleomycin-induced pulmonary fibrosis *in vivo* model. The BLM-induced fibrosis is one of the most accepted models of IPF.[38] Compounds **40** (dosed at 1, 3, and 10 mg/kg BID) and **48** (3, 10, and 30 mg/kg BID) were therefore evaluated in a prophylactic setting, together with the reference compound pirfenidone (dosed at 50 mg/kg BID), an approved treatment for IPF.[39] In this model, BLM was dosed intranasally to mice. Pirfenidone or an S1P2 antagonist was administered twice a day orally for 14 days. The efficacy of the treatments was evaluated by assessing the histopathological changes in lung architecture. To this end, the modification of the Ashcroft score introduced by Matsuse was used.[40,41] After 14 days, administration of BLM caused widespread epithelial damage, inflammation in the lungs, fibrosis, and lung structural distortion, as evidenced by the Ashcroft score in the vehicle groups (orange squares and dots, Figure 7). Pirfenidone and compounds **40** and **48** displayed a marked protective effect at all dosed tested, resulting in statistically significant reduction of the Ashcroft score.

A steady-state PK study was performed on the doses of 3 and 10 mg/kg BID for compound **40**. The exposures appeared to be in both cases well above the IC_{50} values obtained from the IL8 assay (Figure S1, Supporting Information).

As both compounds showed very good activity in the BLM model, **40** and **48** were both engaged in rat toxicology studies. After analysis of the toxicological profiles and ensuing therapeutic windows, compound **40** was selected for further progression.

https://doi.org/10.1021/acs.jmedchem.1c00138
J. Med. Chem. 2021, 64, 6037−6058

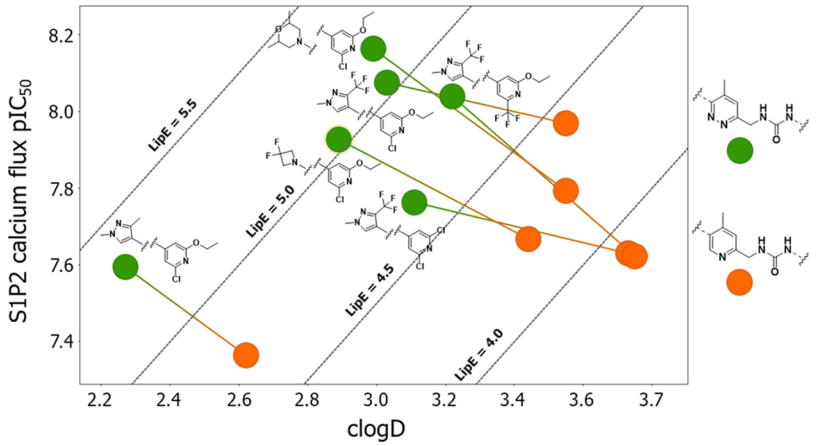

Figure 5. Lipophilicity vs pIC_{50} (calcium flux) for matched pairs between pyridine and pyridazine series.

Table 5. Pharmacokinetics in Preclinical Species and Selected *In Vitro* Data for 37, 40, and 48[a]

	iv PK preclinical species (dose: 1 mg/kg)[b]					thermodynamic solubility	
cpd	species	$t_{1/2}$ (h)	Cl (L/h/kg)	Vss (L/kg)	F (po dose)	PPB (% bound)[g]	FaSSGF (μg/mL)	FaSSIF (μg/mL)
37	mouse	0.55	0.62	0.49	20% (5 mg/kg)[c]	99.8	5	36
	rat	1.1	0.25	0.38	10% (5 mg/kg)[d]	99.9		
	dog	3.1	0.47	2.1	30% (5 mg/kg)[e]	98.4		
40	mouse	2.3	0.24	0.81	64% (5 mg/kg)[d]	99.9	2.7	23
	rat[f]	2.7	0.091	0.35	29% (5 mg/kg)[d]	>99.9		
	dog	7.6	0.10	1.1	100% (5 mg/kg)[e]	99.7		
48	mouse	0.45	0.73	0.47	29% (5 mg/kg)[d]	98.6	505	15
	rat	1.0	0.37	0.54	84% (10 mg/kg)[d]	99.6		
	dog	1.6	0.66	1.5	39% (1 mg/kg)[d]	97.8		

[a]Male CD1 mice (n = 6), male Sprague Dawley rats (n = 3, unless otherwise stated), and male Beagle dogs (n = 3) were used in these studies. Numbers of animals are referring to each study. All values were obtained from plasma. [b]Vehicle was PEG200/water (60/40; v/v). [c]Vehicle was Tween 80/MC 0.5%. [d]Vehicle was PEG400/MC 0.5%. [e]Vehicle was MC 0.5%. [f]n = 2 for the iv route. [g]4 h incubation at a 5 μM compound concentration in plasma.

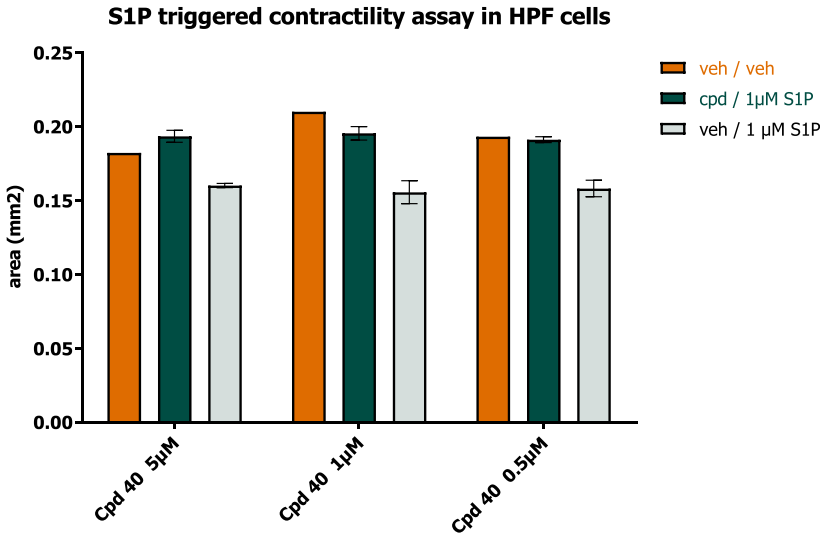

Figure 6. Activity of compound **40** in a cell contraction assay in HPF cells. S1P was used as trigger at 1 μM. Bar height: mean values. Error bars: 95% CI.

Compound **40** displayed no hERG inhibition and limited CYP inhibition and had no liabilities in terms of chemical or plasma stability (Tables S5–S8, Supporting Information). No genotoxicity was detected. **40** was therefore nominated as a preclinical candidate (GLPG2938) for treatment in IPF. Subsequent CMC work in preclinical development resulted in the production of amorphous batches, which resulted in improved solubility. This allowed the smooth running of dose-ranging studies in dogs and rats.

https://doi.org/10.1021/acs.jmedchem.1c00138
J. Med. Chem. 2021, 64, 6037–6058

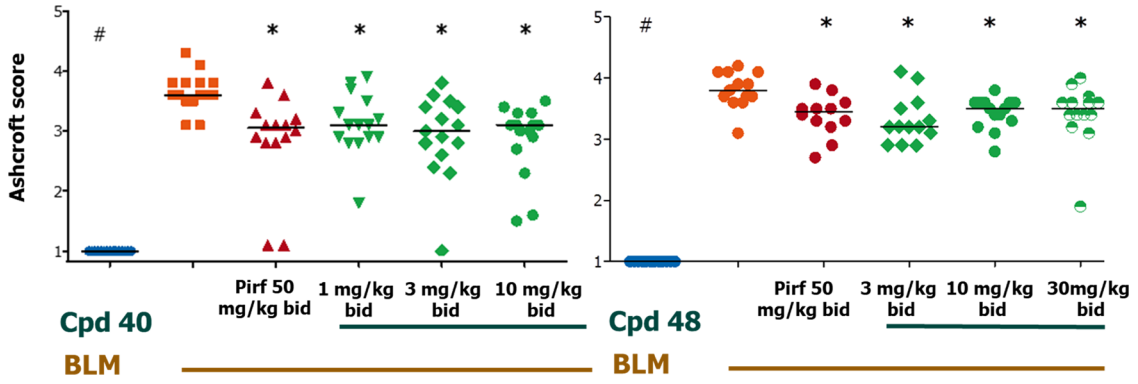

Figure 7. Ashcroft score at D14 following intranasal bleomycin challenge. Data are given as group median. *p < 0.05 vs BLM/vehicle control (Mann−Whitney test). #p < 0.05 vs BLM/Vehicle (Wilcoxon signed-rank test); cpd **40**: n = 15 per group; cpd **48**: n = 14 per group. Animals: male C57BL/6 mice (**40**: 8 weeks old on arrival; **48**: 7 weeks old on arrival. One week acclimation).

Scheme 1. Synthesis of Compounds 12−21[a]

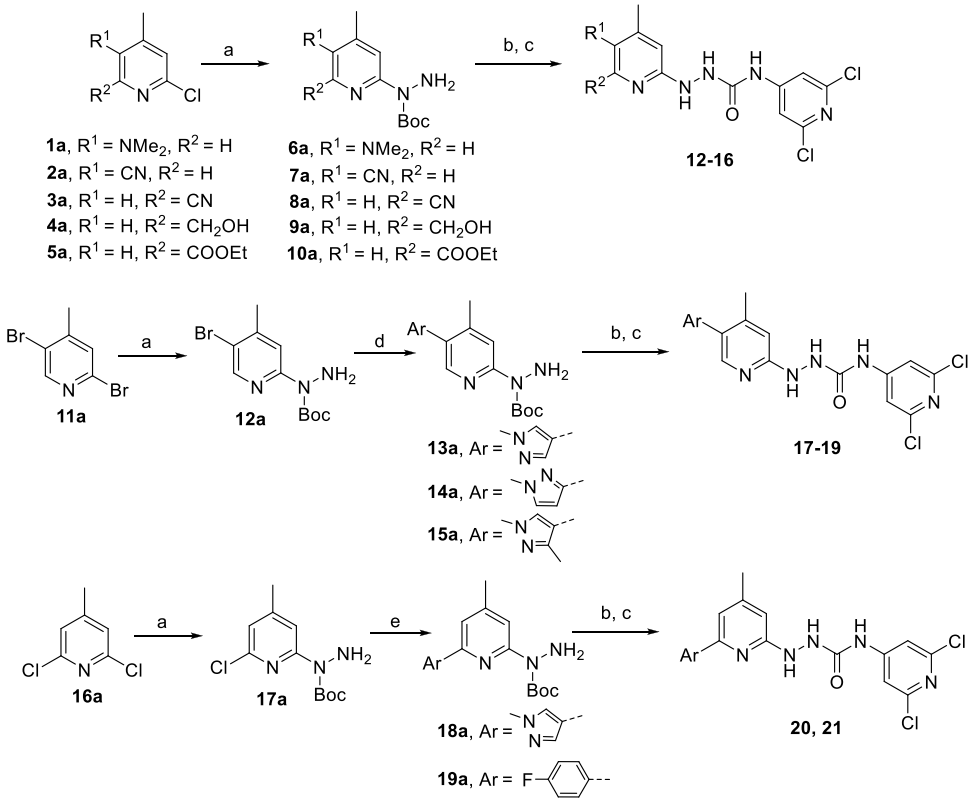

[a]Reagents and conditions: (a) *tert*-butyl hydrazinecarboxylate, Cs_2CO_3, $Pd_2(dba)_3$, dppf, toluene, 100 °C; (b) 2,6-dichloro-4-isocyanatopyridine, THF, rt; (c) 4 M HCl in 1,4-dioxane, DCM, 40 °C; (d) Ar-B(OR)$_2$, 2 M K_2CO_3, Pd(dppf)Cl_2, 1,4-dioxane, 130 °C, μw; (e) Ar-B(OR)$_2$, 2 M Na_2CO_3, Pd(dppf)Cl_2, 1,4-dioxane, 150 °C, μw.

Scheme 2. Synthesis of Compounds 22−24[a]

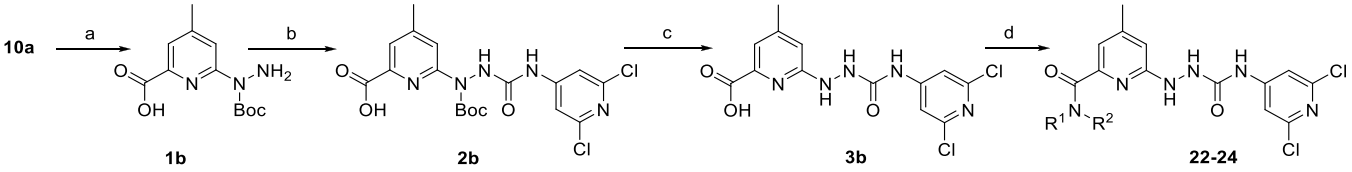

[a]Reagents and conditions: (a) **10a**, LiOH, H_2O/THF; (b) 2,6-dichloro-4-isocyanatopyridine, THF, rt; (c) 4 M HCl in 1,4-dioxane, DCM, 40 °C; (d) R^1R^2NH, HATU, DIPEA, DMF, DCM, rt.

https://doi.org/10.1021/acs.jmedchem.1c00138
J. Med. Chem. 2021, 64, 6037−6058

Scheme 3. Synthesis of Compounds 25 and 27−34[a]

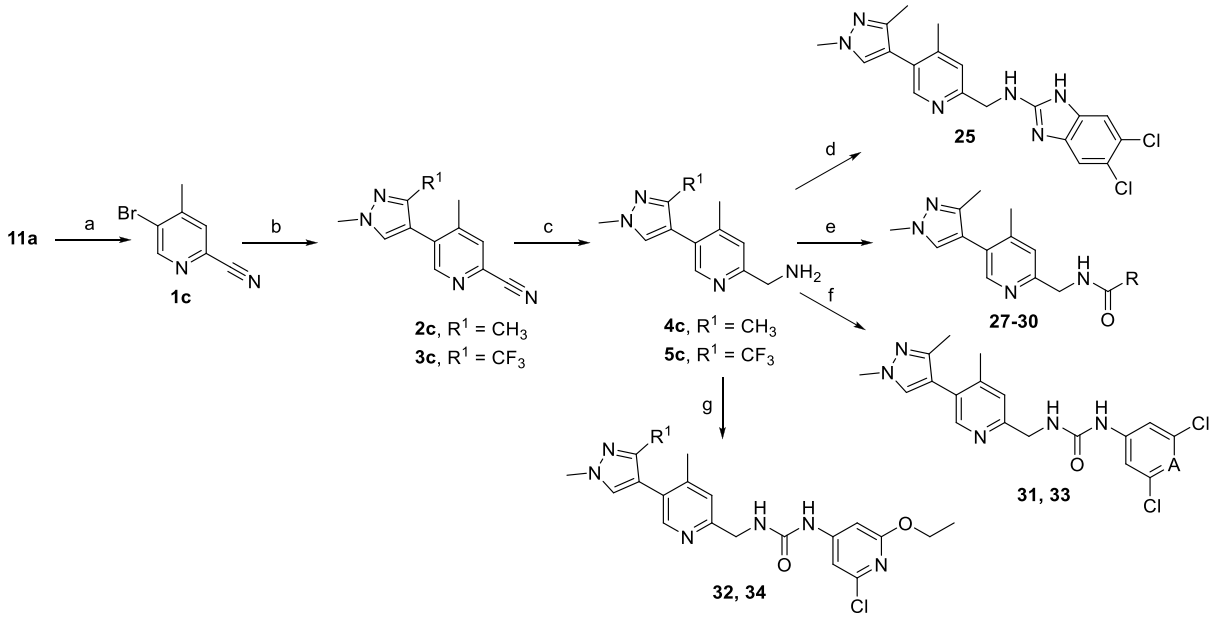

[a]Reagents and conditions: (a) $Zn(CN)_2$, $Pd(PPh_3)_4$, DMF, 150 °C; (b) Ar-$B(OR)_2$, Cs_2CO_3, $Pd(dppf)Cl_2$, 1,4-dioxane, H_2O, 100 °C; (c) $BH_3{\cdot}SMe_2$, THF, 45 °C; (d) 2,5,6-trichloro-1*H*-benzo[*d*]imidazole, MeCN, 170 °C, μw; (e) RCOOH, HATU, DIPEA, DMF, DCM, rt or 45 °C; (f) RNCO, THF, rt; (g) 2-chloro-6-ethoxypyridin-4-amine, CDT, pyridine, DCM, rt.

Scheme 4. Synthesis of Compound 26[a]

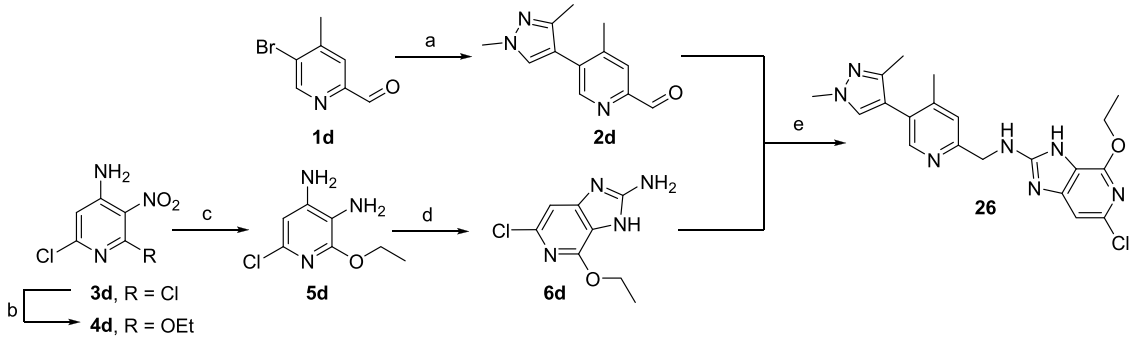

[a]Reagents and conditions: (a) 1,3-dimethyl-4-(4,4,5,5-tetramethyl-1,3,2-dioxaborolan-2-yl)-1*H*-pyrazole, Cs_2CO_3, $Pd(dppf)Cl_2$, 1,4-dioxane, H_2O, 100 °C; (b) EtOH, NaH, rt; (c) Zn, NH_4Cl, MeOH, rt; (d) CNBr, EtOH, 45 °C; (e) $Ti(OiPr)_4$, EtOH, 60 °C.

CHEMISTRY

Final compounds **12−21** were synthesized according to Scheme 1. In summary, Buchwald−Hartwig conditions with *tert*-butyl hydrazinecarboxylate were used to obtain intermediates **6−10a**, **12a**, and **17a** from the respective aryl halides. Intermediates **12a** and **17a** were coupled with aromatic boronic acids/esters to obtain intermediates **13−15a** and **18−19a**. Finally, the hydrazine derivatives **6−10a**, **13−15a**, and **18−19a** underwent a two-step sequence featuring urea formation by reaction with 2,6-dichloro-4-isocyanatopyridine followed by Boc deprotection in acidic medium.

Compounds **22−24** were synthesized according to Scheme 2. Intermediate ester **10a** was hydrolyzed by LiOH to acid **1b**, which underwent urea formation. Final compounds were obtained after Boc deprotection and HATU-based amide coupling with the corresponding amines.

Compounds **25** and **27−34** were synthesized according to Scheme 3. Intermediate **1c** was obtained from **11a** after a regioselective coupling under Negishi conditions. Intermediates **2−3c** were obtained after Suzuki coupling. Reduction of the nitrile group in the presence of $BH_3{\cdot}SMe_2$ yielded primary amine intermediates **4−5c**. S_NAr reaction with 2,5,6-trichloro-1*H*-benzo[*d*]imidazole yielded compound **25**. A series of HATU-mediated couplings between **4c** and the corresponding carboxylic acids delivered compounds **27−30**. Ureas **31** and **33** were obtained after coupling of **4c** with the corresponding isocyanates. Intermediates **4−5c** were coupled with 2-chloro-6-ethoxypyridin-4-amine using 1,1′-carbonyl-di-(1,2,4-triazole) (CDT) to obtain ureas **32** and **34**.

The synthetic sequence described in Scheme 4 led to compound **26**. The bromide **1d** underwent Suzuki coupling with 1,3-dimethyl-4-(4,4,5,5-tetramethyl-1,3,2-dioxaborolan-2-yl)-1*H*-pyrazole to afford intermediate **2d**. Reductive amination with the aminobenzimidazole **6d** gave the desired product **26**. During the optimization of the reductive amination step, it was observed that the reducing agent was not necessary for the reduction of the imine intermediate. It was concluded that the titanium tetraisopropoxide played the roles of both Lewis acid

https://doi.org/10.1021/acs.jmedchem.1c00138
J. Med. Chem. 2021, 64, 6037−6058

Scheme 5. Synthesis of Compound 35[a]

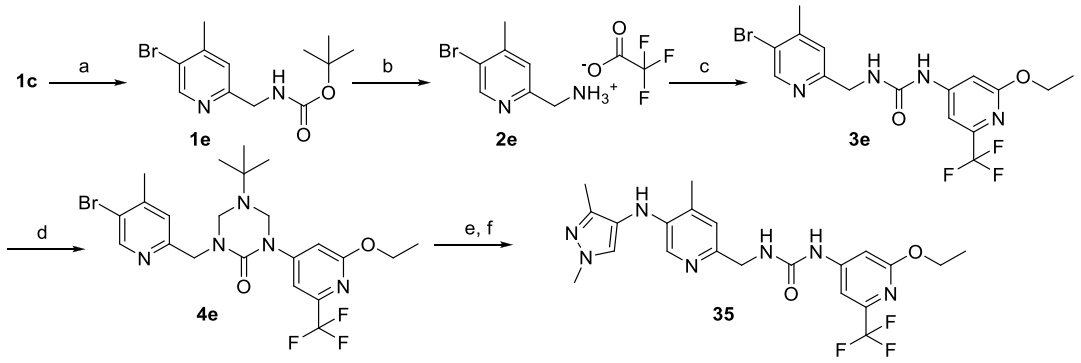

[a]Reagents and conditions: (a) $NaBH_4$, $NiCl_2{\cdot}6H_2O$, Boc_2O, MeOH, rt; (b) TFA, DCM, 45 °C; (c) 2-ethoxy-6-(trifluoromethyl)pyridin-4-amine, CDT, pyridine, DCM, 45 °C; then **2e**, DIPEA, THF, rt; (d) HCHO (37% H_2O), 4-methylmorpholine, *t*$BuNH_2$, EtOH/H_2O, 100 °C; (e) 1,3-dimethyl-1*H*-pyrazol-4-amine, $Pd_2(dba)_3$, BINAP, NaO*t*Bu, toluene, 70 °C; (f) 1,4-dioxane/6 M NaOH, 100 °C.

Scheme 6. Synthesis of Compounds 37−43, 46−48, 50, and 51[a]

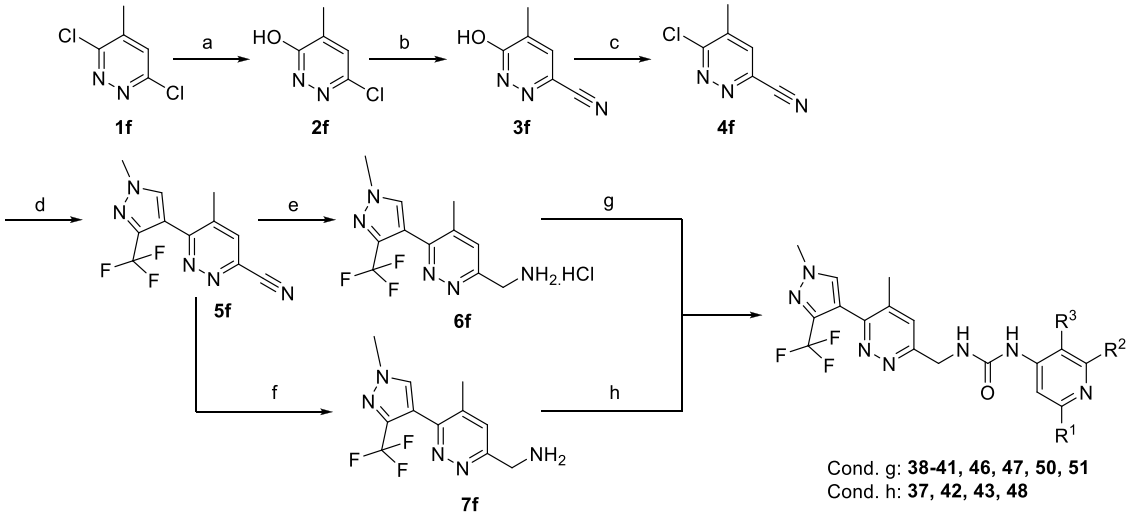

[a]Reagents and conditions (a) 3.3 M NaOH, reflux; (b) $Zn(CN)_2$, $Pd_2(dba)_3$, dppf, DMF, 120 °C; (c) $POCl_3$, MeCN, reflux; (d) 1-methyl-4-(4,4,5,5-tetramethyl-1,3,2-dioxaborolan-2-yl)-3-(trifluoromethyl)-1*H*-pyrazole, $Pd(PPh_3)_4$, DMF, rt; then 2.5 M Na_2CO_3, 85 °C; (e) Pd/C, H_2 gas (1 atm), 6 M HCl, MeOH, rt; (f) $NaBH_4$, TFA, $NiCl_2.6H_2O$, MeOH, rt; (g) RNH_2, CDT, pyridine, DCM, 45 °C; then **6f**, DIPEA, THF, rt; (h) RNH_2, CDT, pyridine, DCM, 45 °C; then **7f**, rt.

and reducing agent in a similar way as the aluminum triisopropoxide does in the Meerwein−Schmidt−Ponndorf−Verley reduction.[42] Compound **122** (Supporting Information, Scheme S31) was also obtained with this procedure. Moreover, a preliminary investigation showed that these conditions were working also on other substrates. Two examples are reported in the Supporting Information (compounds **123** and **124**, Scheme S32). **6d** was synthesized in three steps. The ethoxy group was installed by S_NAr on the bis-chloropyridine **3d** with ethanol. After reduction of the nitro group in **4d** with zinc, the bis-aminopyridine **5d** was cyclized using cyanogen bromide to obtain the 2-aminobenzimidazole **6d**.

Scheme 5 describes the synthesis of compound **35**. Nitrile derivative **1c** (Scheme 3) was reduced and Boc protected in a one-pot procedure to favor purification. Intermediate **2e**, obtained after Boc deprotection from **1e**, was coupled with ethoxy-6-(trifluoromethyl)pyridin-4-amine to form urea **3e**. At this stage, a protecting group based on a 1,3,5-triazinan-2-one was envisaged. The *tert*-butyl group helped for the isolation of the protected urea, ensuring a straightforward chromatographic separation. The strategy adopted here is not widely exploited as we could find only one account for such protecting group applied to a urea bearing an aryl motif.[43] The urea so protected underwent Buchwald−Hartwig coupling with 1,3-dimethyl-1*H*-pyrazol-4-amine. The product was subsequently deprotected in strongly basic conditions to yield the final compound **35**.

The synthesis of compounds **37−43**, **46−48**, **50**, and **51** (Scheme 6) commenced with the hydrolysis of 3,6-dichloro-4-methylpyridazine followed by a Negishi coupling to obtain nitrile **3f**. Chlorination with $POCl_3$ provided **4f**, which was coupled with 1-methyl-4-(4,4,5,5-tetramethyl-1,3,2-dioxaborolan-2-yl)-3-(trifluoromethyl)-1*H*-pyrazole under Suzuki conditions to yield intermediate **5f**. The nitrile group was then reduced using hydrogen gas and palladium on charcoal in the presence of HCl. The acidic environment was necessary to prevent intermolecular attack of the amino group on the partially reduced imine. Alternatively, **5f** could be reduced using a mixture of $NaBH_4$, TFA, and $NiCl_2{\cdot}6H_2O$. The resulting amines **6f** (HCl salt) and **7f** (free base) were coupled

https://doi.org/10.1021/acs.jmedchem.1c00138
J. Med. Chem. 2021, 64, 6037−6058

to the corresponding aminopyridine in the presence of 1,1′-carbonyl-di-(1,2,4-triazole) (CDT) and pyridine to afford the desired products **37**−**43**, **46**−**48**, **50**, and **51**. When the HCl salt **6f** was used, DIPEA as a base on top of pyridine and THF as a co-solvent were necessary to obtain good conversions.

CONCLUSIONS

In this manuscript, we described the discovery of the preclinical candidate GLPG2938 (compound **40**), a novel S1P2 receptor inhibitor possessing high potency, exquisite selectivity, and very good pharmacokinetics. The efficacy obtained in the BLM model at low doses advocated strongly for its progression in development for the treatment of IPF. A key role in this discovery was played by adopting chemical enablement strategies; this allowed us to identify the 5-pyrazol-4-yl-pyridine motif as the key element for further optimization. Chemical enablement also allowed a quick and broad exploration of the space around the pyridine's C5 position. Considerations on lipophilicity were also very important as they led to the pyridazine-based series. This change brought molecules with better LipE and helped to solve a potential CYP inhibition issue.

EXPERIMENTAL SECTION

General Experimental Methods. All reagents were of commercial grade and were used as received without further purification, unless otherwise stated. Commercially available anhydrous solvents were used for reactions conducted under an inert atmosphere. Reagent-grade solvents were used in all other cases, unless otherwise specified. Column chromatography was performed on silica gel 60 (35−70 μm). Thin layer chromatography was carried out using pre-coated silica gel F-254 plates (thickness 0.25 mm). Purification with preparatory HPLC was performed with a Waters FractionLynx system coupled to a 2996 PDA detector and a Waters Mass detector QDA. For the basic method, column used: Waters XBridge prep (C18, 10 μm OBD, 19 x 100 mm); for the acidic method, column used: Waters XSelect CSH (C18, 5 μm OBD, 19 x 100 mm). Flow rate: 20 mL/min. ^{1}H NMR spectra were recorded on a Bruker DPX 400 NMR spectrometer (400 MHz). Chemical shifts (δ) for ^{1}H NMR spectra are reported in parts per million (ppm) relative to tetramethylsilane (δ 0.00) or the appropriate residual solvent peak, i.e., $CHCl_3$ (δ 7.27), as an internal reference. Multiplicities are given as singlet (s), doublet (d), triplet (t), quartet (q), quintuplet (quin), multiplet (m), and broad (br). Ultraviolet and electrospray MS spectra were obtained on a Waters platform LC/MS spectrometer or with Waters Acquity H-Class UPLC coupled to a Waters mass detector QDA. Purities were determined by LCMS analysis (UV traces determined with an Acquity PDA detector) using two methods. Method A: column used: Waters Acquity UPLC CSH C18 1.7 μm, 2.1 mm ID x 50 mm L; MeCN/H_2O gradients (H_2O contains 0.1% formic acid); Method B: column used: Waters Acquity UPLC BEH C18 1.7 μm, 2.1 mm ID x 50 mmL; MeCN/H_2O gradients (H_2O contains 13.4 mM NH_3). All reported final compounds were analyzed with one of these analytical methods and had purities ≥95%.

High-resolution mass spectrometry (HRMS) analyses were performed with a Waters Xevo-G2-XS QTof mass spectrometer coupled to a Waters UPLC H-class system (column: Acquity BEH C18, 100*2.1 mm, 1.7 μm particle size, elution: formic acid 0.1% in water/formic acid 0.1% in acetonitrile 95:5 to 5:95 in 5.2 min, flow: 0.8 mL/min) equipped with a PDA detector (UV detection: total absorbance 210−400 nm), a column heater module, and controlled by Masslynx Software. Microwave heating was performed with a Biotage Initiator. The melting points were measured with a Mettler Toledo, MP50 melting point system.

General Procedure for Preparation of Boc-Protected 2-Hydrazineylpyridines 6−10a, 12a, and 17a. *tert-Butyl 1-(5-Bromo-4-methylpyridin-2-yl)hydrazine-1-carboxylate (**12a**).* $Pd_2(dba)_3$ (334 mg, 0.365 mmol, 0.05 eq) and dppf (606 mg, 1.09 mmol, 0.15 eq) were added to a degassed solution of 2,5-dibromo-4-methylpyridine **11a** (1.83 g, 7.29 mmol, 1.0 eq), *tert*-butyl hydrazinecarboxylate (963 mg, 7.29 mmol, 1.0 eq), and Cs_2CO_3 (2.38 g, 7.29 mmol, 1.0 eq) in dry toluene (36 mL, 0.2 M). The reaction mixture was stirred at 100 °C for 2.5 h. The reaction was cooled down to room temperature and filtered over Celite. The filtrate was washed with saturated aqueous $NaHCO_3$ solution. The compound was extracted with DCM, and the organic layer was dried over $MgSO_4$, filtered, and concentrated to dryness. The crude material was purified by column chromatography (SiO_2, petroleum ether/EtOAc, 100:0 to 0:100 over 20 CV) to afford *tert*-butyl 1-(5-bromo-4-methylpyridin-2-yl)hydrazine-1-carboxylate (1.07 g, 44% yield). LCMS: m/z = 302.0, 304.0 $(M + H)^+$.

*tert-Butyl N-Amino-N-[5-(dimethylamino)-4-methyl-2-pyridyl]-carbamate (**6a**).* This compound was prepared from **1a** according to the general procedure used for the preparation of **12a**. LCMS: m/z = 267.1 $(M + H)^+$.

*tert-Butyl N-Amino-N-(5-cyano-4-methyl-2-pyridyl)carbamate (**7a**).* This compound was prepared from **2a** according to the general procedure used for the preparation of **12a**. LCMS: m/z = 193.2 $((M - 56) + H)^+$.

*tert-Butyl N-Amino-N-(6-cyano-4-methyl-2-pyridyl)carbamate (**8a**).* This compound was prepared from **3a** according to the general procedure used for the preparation of **12a**. LCMS: m/z = 249.0 $(M + H)^+$.

*tert-Butyl N-Amino-N-[6-(hydroxymethyl)-4-methyl-2-pyridyl]-carbamate (**9a**).* This compound was prepared from **4a** according to the general procedure used for the preparation of **12a**. LCMS: m/z = 254.0 $(M + H)^+$.

*Ethyl 6-[Amino(tert-butoxycarbonyl)amino]-4-methylpyridine-2-carboxylate (**10a**).* This compound was prepared from **5a** according to the general procedure used for the preparation of **12a**. LCMS: m/z = 296.0 $(M + H)^+$.

*tert-Butyl N-Amino-N-(6-chloro-4-methyl-2-pyridyl)carbamate (**17a**).* This compound was prepared from **16a** according to the general procedure used for the preparation of **12a**. LCMS: m/z = 258.0 $(M + H)^+$.

General Procedure for Preparation of Boc-Protected 2-Hydrazineylpyridines 13−15a. *tert-Butyl N-Amino-N-[5-(1,3-dimethylpyrazol-4-yl)-4-methyl-2-pyridyl]carbamate (**15a**).* To a degassed solution of *tert*-butyl *N*-amino-*N*-(5-bromo-4-methyl-2-pyridyl)carbamate **12a** (200 mg, 0.661 mmol, 1.0 eq), 1,3-dimethyl-4-(4,4,5,5-tetramethyl-1,3,2-dioxaborolan-2-yl)-1*H*-pyrazole (221 mg, 0.993 mmol, 1.5 eq), and K_2CO_3 (2 M in H_2O, 1.1 mL, 2.3 mmol, 3.5 eq) in 1,4-dioxane (7 mL, 0.1 M) was added Pd(dppf)Cl_2 (27 mg, 0.033 mmol, 0.05 eq), and the reaction was stirred at 130 °C under microwave irradiation until reaction completion. It was then cooled to room temperature and partitioned between saturated aqueous $NaHCO_3$ and DCM. The compound was extracted using a phase separator, and the organic layer was concentrated to dryness to obtain compound **15a**, which was used without further purification. LCMS: m/z = 318.1 $(M + H)^+$.

*tert-Butyl N-Amino-N-[4-methyl-5-(1-methylpyrazol-4-yl)-2-pyridyl]carbamate (**13a**).* This compound was prepared from **12a** according to the general procedure used for the preparation of **15a**. LCMS: m/z = 304.1 $(M + H)^+$.

*tert-Butyl N-Amino-N-[4-methyl-5-(1-methylpyrazol-3-yl)-2-pyridyl]carbamate (**14a**).* This compound was prepared from **12a** according to the general procedure used for the preparation of **15a**. LCMS: m/z = 304.1 $(M + H)^+$.

General Procedure for Preparation of Boc-Protected 2-Hydrazineylpyridines 18−19a. *tert-Butyl N-Amino-N-[6-(4-fluorophenyl)-4-methyl-2-pyridyl]carbamate (**19a**).* To a degassed solution of *tert*-butyl 1-(6-chloro-4-methylpyridin-2-yl)hydrazine-1-carboxylate **17a** (200 mg, 0.776 mmol, 1.0 eq), (4-fluorophenyl)-boronic acid (163 mg, 1.16 mmol, 1.5 eq), and Na_2CO_3 (2 M in H_2O, 1.36 mL, 2.72 mmol, 3.5 eq) in 1,4-dioxane (5 mL, 0.15 M) was added Pd(dppf)Cl_2 (32 mg, 0.04 mmol, 0.05 eq), and the reaction was stirred at 150 °C under microwave irradiation until reaction

https://doi.org/10.1021/acs.jmedchem.1c00138
J. Med. Chem. 2021, 64, 6037−6058

completion. It was then cooled to room temperature and partitioned between saturated aqueous $NaHCO_3$ and DCM. The compound was extracted using a phase separator, and the organic layer was concentrated to dryness to obtain compound **19a**, which was used without further purification. LCMS: m/z = 318.1 $(M + H)^+$.

*tert-Butyl N-Amino-N-[4-methyl-6-(1-methylpyrazol-4-yl)-2-pyridyl]carbamate (**18a**).* This compound was prepared from **17a** according to the general procedure used for the preparation of **19a**. LCMS: m/z = 304.2 $(M + H)^+$.

General Procedure for Preparation of Ureas 12−21. *2-(5-Cyano-4-methylpyridin-2-yl)-N-(2,6-dichloropyridin-4-yl)-hydrazine-1-carboxamide (**13**).* 2,6-Dichloro-4-isocyanatopyridine (0.10 mL, 0.81 mmol, 1 eq) in THF was added to a mixture of *N*-amino-*N*-(5-cyano-4-methyl-2-pyridyl)carbamate **7a** (200 mg, 0.81 mmol, 1 eq) in THF (8 mL final volume). The reaction was stirred at room temperature until the disappearance of the starting material (4 h). The mixture was partitioned between DCM and water. The two phases were separated; the organic layer was dried (filtered through phase separator) and concentrated. The residue was taken up in DCM (8 mL), and 4 M HCl in 1,4-dioxane (2.0 mL, 8.1 mmol, 10 eq) was added to the mixture. The reaction was stirred at 40 °C until completion (1.5 h). The reaction was quenched with saturated $NaHCO_3$, and the two layers were separated. The aqueous layer was further extracted with DCM. The combined organic layers were dried (filtered through phase separator) and concentrated. The residue was purified by preparatory HPLC (gradient from 30% MeCN to 55% MeCN in water/0.1% formic acid) to obtain the title product (11 mg, 4% yield). LCMS: method A, R_t: 1.16 min; purity: >99%, m/z = 336.9 $(M + H)^+$. ^{1}H NMR (400 MHz, DMSO-d_6) δ 9.78 (s, 1H), 9.22 (s, 1H), 8.99 (s, 1H), 8.45 (s, 1H), 7.68 (s, 2H), 6.64 (s, 1H), 2.38 (s, 3H).

*1-(2,6-Dichloro-4-pyridyl)-3-[[5-(dimethylamino)-4-methyl-2-pyridyl]amino]urea (**12**).* This compound was prepared from **6a** according to the general procedure used for the preparation of **13**. LCMS: method A, R_t: 0.90 min; purity: >99%, m/z = 355.0 $(M + H)^+$. ^{1}H NMR (400 MHz, DMSO-d_6) δ 9.65 (s, 1H), 8.80 (s, 1H), 8.03 (s, 1H), 7.84 (s, 2H), 6.50 (s, 1H), 2.60 (s, 6H), 2.21 (s, 3H).

*1-[(6-Cyano-4-methyl-2-pyridyl)amino]-3-(2,6-dichloro-4-pyridyl)urea (**14**).* This compound was prepared from **8a** according to the general procedure used for the preparation of **13**. LCMS: method B, R_t: 1.20 min; purity: >99%, m/z = 337.0 $(M + H)^+$. ^{1}H NMR (400 MHz, DMSO-d_6) δ 9.74 (s, 1H), 8.95−8.91 (m, 2H), 7.72 (s, 2H), 7.25 (s, 1H), 6.79 (s, 1H), 2.29 (s, 3H).

*1-(2,6-Dichloro-4-pyridyl)-3-[[6-(hydroxymethyl)-4-methyl-2-pyridyl]amino]urea (**15**).* This compound was prepared from **9a** according to the general procedure used for the preparation of **13**. LCMS: method A, R_t: 0.87 min; purity: >99%, m/z = 342.0 $(M + H)^+$. ^{1}H NMR (400 MHz, DMSO-d_6) δ 9.77 (s, 1H), 8.88 (s, 1H), 7.76 (s, 2H), 6.78 (s, 1H), 6.44 (s, 1H), 4.42 (s, 2H), 2.27 (s, 3H).

*Ethyl 6-[2-[(2,6-Dichloro-4-pyridyl)carbamoyl]hydrazino]-4-methylpyridine-2-carboxylate (**16**).* This compound was prepared from **10a** according to the general procedure used for the preparation of **13**. LCMS: method A, R_t: 1.28 min; purity: >99%, m/z = 384.1 $(M + H)^+$. ^{1}H NMR (400 MHz, DMSO-d_6) δ 9.84 (s, 1H), 8.94 (s, 1H), 8.70 (s, 1H), 7.66 (s, 2H), 7.33 (s, 1H), 6.73 (s, 1H), 4.30 (q, J = 7.1 Hz, 2H), 2.32 (s, 3H), 1.29 (t, J = 7.1 Hz, 3H).

*1-(2,6-Dichloro-4-pyridyl)-3-[[4-methyl-5-(1-methylpyrazol-4-yl)-2-pyridyl]amino]urea (**17**).* This compound was prepared from **13a** according to the general procedure used for the preparation of **13**. LCMS: method A, R_t: 0.94 min; purity: >99%, m/z = 392.0 $(M + H)^+$. ^{1}H NMR (400 MHz, DMSO-d_6) δ 9.68 (s, 1H), 8.90 (s, 1H), 8.32 (s, 1H), 8.07 (s, 1H), 7.90 (s, 2H), 7.62 (s, 1H), 6.57 (s, 1H), 3.87 (s, 3H), 2.29 (s, 3H).

*1-(2,6-Dichloro-4-pyridyl)-3-[[4-methyl-5-(1-methylpyrazol-3-yl)-2-pyridyl]amino]urea (**18**).* This compound was prepared from **14a** according to the general procedure used for the preparation of **13**. LCMS: method A, R_t: 0.99 min; purity: >99%, m/z = 392.0 $(M + H)^+$. ^{1}H NMR (400 MHz, DMSO-d_6) δ 8.89 (s, 1H), 8.39 (s, 1H), 8.23−8.20 (m, 1H), 7.87 (s, 1H), 7.73 (s, 1H), 6.78 (s, 1H), 6.56 (s, 1H), 6.50 (s, 1H), 6.46 (s, 1H), 3.87 (s, 3H), 2.39 (s, 3H).

*1-(2,6-Dichloro-4-pyridyl)-3-[[5-(1,3-dimethylpyrazol-4-yl)-4-methyl-2-pyridyl]amino]urea (**19**).* This compound was prepared from **15a** according to the general procedure used for the preparation of **13**. LCMS: method A, R_t: 0.95 min; purity: >99%, m/z = 406.1 $(M + H)^+$. ^{1}H NMR (400 MHz, DMSO-d_6) δ 9.70 (s, 1H), 8.81 (s, 1H), 8.32 (s, 1H), 8.02−7.46 (m, 4H), 6.59 (s, 1H), 3.78 (s, 3H), 2.12 (s, 3H), 2.03 (s, 3H).

*1-(2,6-Dichloro-4-pyridyl)-3-[[4-methyl-6-(1-methylpyrazol-4-yl)-2-pyridyl]amino]urea (**20**).* This compound was prepared from **18a** according to the general procedure used for the preparation of **13**. LCMS: method A, R_t: 1.11 min; purity: >99%, m/z = 392.1 $(M + H)^+$. ^{1}H NMR (400 MHz, DMSO-d_6) δ 10.11 (s, 1H), 9.12 (s, 1H), 8.38 (s, 1H), 8.10 (s, 1H), 7.70 (s, 2H), 7.14 (s, 1H), 6.63 (s, 1H), 3.91 (s, 3H), 2.34 (s, 3H).

*1-(2,6-Dichloro-4-pyridyl)-3-[[6-(4-fluorophenyl)-4-methyl-2-pyridyl]amino]urea (**21**).* This compound was prepared from **19a** according to the general procedure used for the preparation of **13**. LCMS: method A, R_t: 1.44 min; purity: >99%, m/z = 406.6 $(M + H)^+$. ^{1}H NMR (400 MHz, DMSO-d_6) δ 9.76 (s, 1H), 8.85 (s, 1H), 8.42 (s, 1H), 8.11−8.03 (m, 2H), 7.84 (s, 2H), 7.27 (t, J = 8.9 Hz, 3H), 6.48 (s, 1H), 2.31 (s, 3H).

*6-[Amino(tert-butoxycarbonyl)amino]-4-methylpyridine-2-carboxylic acid (**1b**).* A solution of LiOH (1.8 g, 43 mmol, 2.8 eq) in H_2O (15 mL) was added to a mixture of ethyl 6-[amino(*tert*-butoxycarbonyl)amino]-4-methylpyridine-2-carboxylate **10a** (4.4 g, 15 mmol, 1 eq) in THF (30 mL). The reaction was stirred for 2 h at room temperature. The reaction mixture was acidified and extracted with DCM. The two phases were separated. The organic layer was dried (filtered through phase separator) and concentrated to afford the desired product (3 g, 75% yield). LCMS: m/z = 268.1 $(M + H)^+$.

*6-[tert-Butoxycarbonyl-[(2,6-dichloro-4-pyridyl)-carbamoylamino]amino]-4-methylpyridine-2-carboxylic acid (**2b**).* 2,6-Dichloro-4-isocyanatopyridine (1.4 mL, 11 mmol, 1 eq) in THF was added to a mixture of *N*-amino-*N*-(5-cyano-4-methyl-2-pyridyl)-carbamate **1b** (2.9 g, 11 mmol, 1 eq) in THF (110 mL final volume). The reaction was stirred at room temperature until the disappearance of the starting material (2.5 h). The mixture was partitioned between DCM and water. The two phases were separated; the organic layer was dried (filtered through phase separator) and concentrated to afford the desired product (4.2 g, 84% yield). LCMS: m/z = 456.1 $(M + H)^+$.

*6-[2-[(2,6-Dichloro-4-pyridyl)carbamoyl]hydrazino]-4-methylpyridine-2-carboxylic acid (**3b**).* A 4 M HCl solution in 1,4-dioxane (23 mL, 92 mmol, 10 eq) was added to a mixture of 6-[*tert*-butoxycarbonyl-[(2,6-dichloro-4-pyridyl)carbamoylamino]amino]-4-methylpyridine-2-carboxylic acid **2b** (4.2 g, 9.2 mmol, 1 eq) in DCM (92 mL). The resulting mixture was stirred at 40 °C for 2 h. The mixture was concentrated, and the residue was washed with methyl *tert*-butyl ether to afford the desired product (3.0 g, 92% yield). LCMS: m/z = 356.0 $(M + H)^+$.

General Procedure for Preparation of Amides 22−24. *N-Cyclopropyl-6-[2-[(2,6-dichloro-4-pyridyl)carbamoyl]hydrazino]-4-methylpyridine-2-carboxamide (**23**).* A solution of HATU (53 mg, 0.14 mmol, 1 eq) in dry DMF (1 mL) was added to a mixture of cyclopropanamine (8.8 mg, 0.154 mmol, 1.1 eq), 6-[2-[(2,6-dichloro-4-pyridyl)carbamoyl]hydrazino]-4-methylpyridine-2-carboxylic acid **3b** (50 mg, 0.14 mmol, 1 eq), and DIPEA (50 μL, 0.28 mmol, 2 eq) in dry DCM (1.4 mL). The reaction was stirred at room temperature until full conversion. The reaction mixture was quenched with saturated $NaHCO_3$, and the resulting mixture was extracted with DCM. The two phases were separated. The organic layer was dried (filtered through phase separator) and concentrated. The residue was purified by preparatory HPLC (gradient from 35% MeCN to 60% MeCN in water/0.1% formic acid) to afford the desired product (5 mg, 10% yield). LCMS: method B, R_t: 1.21 min; purity: >99%, m/z = 356.0 $(M + H)^+$. ^{1}H NMR (400 MHz, DMSO-d_6) δ 9.84 (s, 1H), 8.86 (s, 1H), 8.52 (s, 1H), 8.04 (d, J = 4.6 Hz, 1H), 7.83−7.54 (m, 2H), 7.26 (s, 1H), 6.67 (s, 1H), 2.87−2.76 (m, 1H), 2.31 (s, 3H), 0.79−0.64 (m, 2H), 0.50−0.42 (m, 2H).

*6-[2-[(2,6-Dichloro-4-pyridyl)carbamoyl]hydrazino]-N,N,4-trimethylpyridine-2-carboxamide (**22**).* This compound was prepared

https://doi.org/10.1021/acs.jmedchem.1c00138
J. Med. Chem. 2021, 64, 6037−6058

from **3b** according to the general procedure used for the preparation of **23**. LCMS: method B, R_t: 1.14 min; purity: 95%, m/z = 383.0 (M + H)$^+$. ^{1}H NMR (400 MHz, DMSO-d_6) δ 8.94 (s, 1H), 8.49 (s, 1H), 7.80 (s, 3H), 6.76 (s, 2H), 6.54 (s, 1H), 6.50 (s, 1H), 2.93 (s, 3H), 2.88 (s, 3H), 2.27 (s, 3H).

*N-Cyclopropyl-6-[2-[(2,6-dichloro-4-pyridyl)carbamoyl]-hydrazino]-N,4-dimethylpyridine-2-carboxamide (**24**).* This compound was prepared from **3b** according to the general procedure used for the preparation of **23**. LCMS: method B, R_t: 1.22 min; purity: >99%, m/z = 409.1 (M + H)$^+$. ^{1}H NMR (400 MHz, DMSO-d_6) δ 9.68 (s, 1H), 8.79 (s, 1H), 8.53 (s, 1H), 7.66 (d, J = 119.1 Hz, 2H), 6.76 (s, 1H), 6.54 (s, 1H), 2.90 (s, 3H), 2.81−2.75 (m, 1H), 2.27 (s, 3H), 0.43−0.12 (m, 4H).

*5-(1,3-Dimethylpyrazol-4-yl)-4-methylpyridine-2-carbaldehyde (**2d**).* Pd(dppf)Cl$_2$ (204 mg, 0.25 mmol, 0.1 eq) was added to a degassed mixture of 1,3-dimethyl-4-(4,4,5,5-tetramethyl-1,3,2-dioxaborolan-2-yl)-1*H*-pyrazole (670 mg, 3.0 mmol, 1.2 eq), 5-bromo-4-methylpicolinaldehyde **1d** (500 mg, 2.5 mmol, 1 eq), and Cs_2CO_3 (2.04 g, 6.25 mmol, 2.5 eq) in 10:1 1,4-dioxane/H_2O (12 mL). The reaction was stirred at 95 °C for 4 h. The mixture was filtered through Celite. The filtrate was partitioned between DCM and H_2O. The two phases were separated. The aqueous layer was extracted with DCM. The combined organic layers were dried (filtered through a phase separator) and concentrated to afford the desired product (363 mg, 68% yield). LCMS: m/z = 216.1 (M + H)$^+$.

*6-Chloro-2-ethoxy-3-nitropyridin-4-amine (**4d**).* NaH in 60% mineral oil (154 mg, 3.84 mmol, 2 eq) was added to a mixture of 2,6-dichloro-3-nitropyridin-4-amine **3d** (400 mg, 1.92 mmol, 1 eq) in EtOH (6.4 mL). The reaction was stirred at room temperature for 1 h. Water was added, and the resulting mixture was extracted with DCM. The two phases were separated. The organic layer was dried (filtered through phase separator) and concentrated to afford the desired product, which was used as such in the next step. LCMS: m/z = 218.0 (M + H)$^+$.

*6-Chloro-2-ethoxypyridine-3,4-diamine (**5d**).* Zn dust (1.5 g, 23 mmol, 12 eq) and NH_4Cl (1.23 g, 23 mmol, 12 eq) were added to a mixture of 6-chloro-2-ethoxy-3-nitropyridin-4-amine **4d** (1.92 mmol, 1 eq) in MeOH (13 mL). The reaction was stirred at room temperature for 2.5 h. The mixture was filtered through Celite and concentrated. The residue was taken up in DCM. The resulting mixture was washed with saturated $NaHCO_3$. The two phases were separated. The organic layer was dried (filtered through a phase separator) and concentrated to afford the desired product, which was used as such in the next step. LCMS: m/z = 188.0 (M + H)$^+$.

*6-Chloro-4-ethoxy-3H-imidazo[4,5-c]pyridin-2-amine (**6d**).* CNBr (5 M MeCN solution, 1 mL, 5.8 mmol, 3 eq) was added to a mixture of 6-chloro-4-ethoxy-3*H*-imidazo[4,5-*c*]pyridin-2-amine **5d** (1.9 mmol, 1 eq) in EtOH (3.8 mL). The mixture was stirred at 45 °C overnight. The mixture was concentrated. The residue was taken up in EtOAc. The organic mixture was washed with saturated $NaHCO_3$, and the two phases were separated. The aqueous layer was extracted with EtOAc. The combined organic layers were dried (Na_2SO_4), filtered, and concentrated to afford the desired product (50 mg, 12% yield). LCMS: m/z = 213.0 (M + H)$^+$.

*6-Chloro-N-[[5-(1,3-dimethylpyrazol-4-yl)-4-methyl-2-pyridyl]-methyl]-4-ethoxy-3H-imidazo[4,5-c]pyridin-2-amine (**26**).* Ti(O*i*Pr)$_4$ (0.21 mL, 0.705 mmol, 3 eq) was added to a mixture of 6-chloro-4-ethoxy-3*H*-imidazo[4,5-*c*]pyridin-2-amine **6d** (50 mg, 0.24 mmol, 1 eq) and 5-(1,3-dimethylpyrazol-4-yl)-4-methylpyridine-2-carbaldehyde **2d** (101 mg, 0.47 mmol, 2 eq) in EtOH (0.5 mL). The reaction was stirred at 60 °C overnight. The mixture was diluted with MeOH. Na_2SO_4·10H_2O was added, and the mixture was stirred for 30 min. The mixture was filtered, and the filtrate was concentrated. The residue was taken up in EtOAc and washed with 1 M NaOH. The two phases were separated. The organic layer was dried (Na_2SO_4) and concentrated. The residue was purified by preparatory HPLC (gradient from 20% MeCN to 45% MeCN in water/0.1% formic acid) to afford the desired product (3.0 mg, 3% yield). LCMS: method B, R_t: 1.16 min; purity: >99%, m/z = 412.2 (M + H)$^+$. ^{1}H NMR (400 MHz, DMSO-d_6) δ 11.56 (s, 1H), 8.26 (s, 1H), 7.73 (s, 1H), 7.44 (s, 1H), 7.26 (s, 1H), 6.88 (s, 1H), 4.61 (d, J = 5.9 Hz, 2H), 4.36 (s, 2H), 3.80 (s, 3H), 2.18 (s, 3H), 2.06 (s, 3H), 1.35 (t, J = 7.1 Hz, 3H).

*5-Bromo-4-methylpyridine-2-carbonitrile (**1c**).* A mixture of 2,5-dibromo-4-methylpyridine **11a** (5 g, 20 mmol, 1 eq), $Zn(CN)_2$ (2.81 g, 23.9 mmol, 1.2 eq) and $Pd(PPh_3)_4$ (2.3 g, 2.0 mmol, 0.1 eq) in DMF (100 mL) was heated at 150 °C under microwave irradiation for 5 min. The mixture was filtered through Celite. The filtrate was diluted with DCM. The resulting mixture was washed (sat $NaHCO_3$ and brine), dried (filtered through a phase separator) and concentrated. The residue was purified by flash column chromatography (SiO_2, 95:5 petroleum ether/EtOAc) to afford the desired product (4.4 g, 100% yield). LCMS: m/z = 198.9 (M + H)$^+$.

General Procedure for Preparation of Nitriles 2−3c. *5-(1,3-Dimethylpyrazol-4-yl)-4-methylpyridine-2-carbonitrile (**2c**).* Pd(dppf)Cl$_2$ (415 mg, 0.51 mmol, 0.1 eq) was added to a degassed mixture containing 5-bromo-4-methylpyridine-2-carbonitrile **1c** (1.0 g, 5.1 mmol, 1 eq), 1,3-dimethyl-4-(4,4,5,5-tetramethyl-1,3,2-dioxaborolan-2-yl)-1*H*-pyrazole (1.35 g, 6.09 mmol, 1.2 eq), and Cs_2CO_3 (4.10 g, 12.7 mmol, 2.5 eq) in 4:1 1,4-dioxane/H_2O (20 mL). The reaction mixture was stirred at 100 °C for 2.5 h. The mixture was cooled to room temperature and quenched with H_2O. The resulting mixture was extracted with DCM. The organic layer was dried (filtered through a phase separator) and concentrated to dryness to afford the desired product (550 mg, 51% yield). LCMS: m/z = 213.0 (M + H)$^+$.

*4-Methyl-5-[1-methyl-3-(trifluoromethyl)pyrazol-4-yl]pyridine-2-carbonitrile (**3c**).* This compound was prepared from **1c** according to the general procedure used for the preparation of **2c**. LCMS: m/z = 267.1 (M + H)$^+$.

General Procedure for Preparation of Amines 4−5c. *[5-(1,3-Dimethylpyrazol-4-yl)-4-methyl-2-pyridyl]methanamine (**4c**).* BH_3·SMe_2 (2.4 mL, 25 mmol, 5 eq) was slowly added to a mixture of 5-(1,3-dimethylpyrazol-4-yl)-4-methylpyridine-2-carbonitrile **2c** (1.1 g, 5.1 mmol, 1 eq) in THF at room temperature. The reaction mixture was stirred at 45 °C for 1 h. The mixture was cooled to 0 °C, and MeOH was carefully added. The resulting mixture was concentrated. The residue was taken up in DCM, and 2 M HCl was added. The two phases were separated. The aqueous layer was basified and extracted with DCM. The two phases were separated. The organic layer was dried (filtered through a phase separator) and concentrated to afford the desired product (400 mg, 36% yield). LCMS: m/z = 217.1 (M + H)$^+$.

*[4-Methyl-5-[1-methyl-3-(trifluoromethyl)pyrazol-4-yl]-2-pyridyl]methanamine (**5c**).* This compound was prepared from **3c** according to the general procedure used for the preparation of **4c**. LCMS: m/z = 271.1 (M + H)$^+$.

*5,6-Dichloro-N-[[5-(1,3-dimethylpyrazol-4-yl)-4-methyl-2-pyridyl]methyl]-1H-benzimidazol-2-amine (**25**).* A mixture of [5-(1,3-dimethylpyrazol-4-yl)-4-methyl-2-pyridyl]methanamine **4c** (100 mg, 0.46 mmol, 1.2 eq) and 2,5,6-trichloro-1*H*-benzo[*d*]imidazole (85 mg, 0.39 mmol, 1 eq) in acetonitrile (0.5 mL) was stirred at 170 °C under microwave conditions for 40 min. The mixture was partitioned between DCM and H_2O. The two phases were separated. The organic layer was dried (filtered through phase separator) and concentrated. The residue was purified by preparatory HPLC (gradient from 30% MeCN to 55% MeCN in water/0.5% NH_3) to afford the desired product (7.5 mg, 5% yield). LCMS: method A, R_t: 0.95 min; purity: >99%, m/z = 401.1 (M + H)$^+$. ^{1}H NMR (400 MHz, DMSO-d_6) δ 11.09 (s, 1H), 8.26 (s, 1H), 7.74 (s, 1H), 7.55 (t, J = 6.0 Hz, 1H), 7.32−7.28 (m, 3H), 4.60 (d, J = 5.9 Hz, 2H), 3.80 (s, 3H), 2.18 (s, 3H), 2.06 (s, 3H).

General Procedure for Preparation of Amides 27, 29, and 30. *4,6-Dichloro-N-[[5-(1,3-dimethylpyrazol-4-yl)-4-methyl-2-pyridyl]methyl]-1H-indole-2-carboxamide (**27**).* A solution of HATU (131 mg, 0.35 mmol, 1 eq) in dry DMF (1 mL) was added to a mixture of [5-(1,3-dimethylpyrazol-4-yl)-4-methyl-2-pyridyl]-methanamine **4c** (75 mg, 0.35 mmol, 1 eq), 4,6-dichloro-1*H*-indole-2-carboxylic acid (88 mg, 0.38 mmol, 1.1 eq), and DIPEA (120 μL, 0.69 mmol, 2 eq) in dry DCM (3.5 mL). The reaction was stirred at room

https://doi.org/10.1021/acs.jmedchem.1c00138
J. Med. Chem. 2021, 64, 6037−6058

temperature until full conversion. The reaction mixture was partitioned between DCM and saturated NH_4Cl. The two phases were separated. The organic layer was dried (filtered through phase separator) and concentrated. The residue was purified by preparatory HPLC (gradient from 35% MeCN to 60% MeCN in water/0.1% formic acid) to afford the desired product (2.0 mg, 1% yield). LCMS: method B, R_t: 1.19 min; purity: >99%, m/z = 428.1 $(M + H)^+$. ^1H NMR (400 MHz, DMSO-d_6) δ 12.18 (s, 1H), 9.34 (t, J = 6.0 Hz, 1H), 8.26 (s, 1H), 7.74 (s, 1H), 7.46−7.41 (m, 1H), 7.38 (d, J = 0.9 Hz, 1H), 7.29−7.24 (m, 2H), 4.59 (d, J = 6.0 Hz, 2H), 3.81 (s, 3H), 2.20 (s, 3H), 2.07 (s, 3H).

*2,6-Dichloro-N-[[5-(1,3-dimethylpyrazol-4-yl)-4-methyl-2-pyridyl]methyl]pyridine-4-carboxamide (**29**).* This compound was prepared from **4c** according to the general procedure used for the preparation of **27**. LCMS: method A, R_t: 1.19 min; purity: >99%, m/z = 390.1 $(M + H)^+$. ^1H NMR (400 MHz, Chloroform-d) δ 8.35 (s, 1H), 7.87 (s, 1H), 7.71 (s, 2H), 7.31 (s, 1H), 7.22 (s, 1H), 4.73 (d, J = 4.5 Hz, 2H), 3.94 (s, 3H), 2.29 (s, 3H), 2.19 (s, 3H).

*2-(3,4-Dichlorophenyl)-N-[[5-(1,3-dimethylpyrazol-4-yl)-4-methyl-2-pyridyl]methyl]acetamide (**30**).* This compound was prepared from **4c** according to the general procedure used for the preparation of **27**. LCMS: method A, R_t: 1.23 min; purity: >99%, m/z = 403.1 $(M + H)^+$. ^1H NMR (400 MHz, Chloroform-d) δ 8.27 (s, 1H), 7.48−7.39 (m, 2H), 7.28 (s, 1H), 7.19 (dd, J = 8.2, 2.1 Hz, 1H), 7.15−7.10 (m, 1H), 6.86 (s, 1H), 4.54 (d, J = 5.0 Hz, 2H), 3.93 (s, 3H), 3.61 (s, 2H), 2.24 (d, J = 0.6 Hz, 3H), 2.17 (s, 3H).

*4,6-Dichloro-N-[[5-(1,3-dimethylpyrazol-4-yl)-4-methyl-2-pyridyl]methyl]-1H-pyrrolo[3,2-c]pyridine-2-carboxamide (**28**).* A solution of HATU (131 mg, 0.35 mmol, 1 eq) in dry DMF (1 mL) was added to a mixture of [5-(1,3-dimethylpyrazol-4-yl)-4-methyl-2-pyridyl]methanamine **4c** (75 mg, 0.35 mmol, 1 eq), 4,6-dichloro-1*H*-pyrrolo[3,2-*c*]pyridine-2-carboxylic acid (88 mg, 0.38 mmol, 1.1 eq), and DIPEA (120 μL, 0.69 mmol, 2 eq) in dry DCM (3.5 mL). The reaction was stirred at 45 °C until full conversion. The reaction mixture was partitioned between DCM and saturated NH_4Cl. The two phases were separated. The organic layer was dried (filtered through phase separator) and concentrated. The residue was purified by preparatory HPLC (gradient from 35% MeCN to 60% MeCN in water/0.5% NH_3) to afford the desired product (15 mg, 10% yield). LCMS: method B, R_t: 1.15 min; purity: >99%, m/z = 429.2 $(M + H)^+$. ^1H NMR (400 MHz, DMSO-d_6) δ 12.63 (d, J = 2.1 Hz, 1H), 9.45 (t, J = 6.0 Hz, 1H), 8.26 (s, 1H), 7.74 (s, 1H), 7.47 (dd, J = 2.1, 1.0 Hz, 1H), 7.43 (d, J = 0.9 Hz, 1H), 7.28 (s, 1H), 4.60 (d, J = 5.9 Hz, 2H), 3.81 (s, 3H), 2.20 (s, 3H), 2.06 (s, 3H).

General Procedure for Preparation of Ureas 31 and 33. *1-(2,6-Dichloro-4-pyridyl)-3-[[5-(1,3-dimethylpyrazol-4-yl)-4-methyl-2-pyridyl]methyl]urea (**31**).* 2,6-Dichloro-4-isocyanatopyridine (131 mg, 0.69 mmol, 1 eq) in THF was added to a mixture of [5-(1,3-dimethylpyrazol-4-yl)-4-methyl-2-pyridyl]methanamine **4c** (150 mg, 0.69 mmol, 1 eq) in THF (7 mL final volume). The reaction was stirred at room temperature until the disappearance of the starting material (1.25 h). The mixture was partitioned between DCM and H_2O. The two phases were separated; the organic layer was dried (filtered through phase separator) and concentrated. The residue was purified by preparatory HPLC (gradient from 20% MeCN to 45% MeCN in water/0.1% formic acid) to afford the desired product (2 mg, 1% yield). LCMS: method B, R_t: 1.19 min; purity: >99%, m/z = 405.1 $(M + H)^+$. ^1H NMR (400 MHz, DMSO-d_6) δ 10.05 (s, 1H), 8.25 (s, 1H), 7.73 (s, 1H), 7.58−7.48 (m, 3H), 7.25 (s, 1H), 4.40 (d, J = 5.5 Hz, 2H), 3.81 (s, 3H), 2.21 (s, 3H), 2.06 (s, 3H).

*1-(3,5-Dichlorophenyl)-3-[[5-(1,3-dimethylpyrazol-4-yl)-4-methyl-2-pyridyl]methyl]urea (**33**).* This compound was prepared from **4c** according to the general procedure used for the preparation of **31**. LCMS: method B, R_t: 1.31 min; purity: >99%, m/z = 404.1 $(M + H)^+$. HRMS: calcd mass for $C_{19}H_{20}Cl_2N_5O$ $(M + H)^+$ 404.1039; found 404.1042; difference 0.6 ppm. ^1H NMR (400 MHz, Chloroform-d) δ 8.43 (s, 1H), 8.26 (s, 1H), 7.31−7.24 (m, 4H), 6.92 (s, 1H), 6.79 (s, 1H), 4.54 (s, 2H), 3.91 (s, 3H), 2.26 (s, 3H), 2.14 (s, 3H).

General Procedure for Preparation of Ureas 32 and 34. *1-(2-Chloro-6-ethoxy-4-pyridyl)-3-[[4-methyl-5-[1-methyl-3-(trifluoromethyl)pyrazol-4-yl]-2-pyridyl]methyl]urea (**34**).* A mixture of 2-chloro-6-ethoxypyridin-4-amine (25 mg, 0.15 mmol, 0.5 eq), pyridine (35 μL, 0.44 mmol, 1.5 eq), and 1,1′-carbonyl-di-(1,2,4-triazole) (36 mg, 0.22 mmol, 0.75 eq) in DCM (1.5 mL) was stirred at room temperature for 0.5 h. [4-Methyl-5-[1-methyl-3-(trifluoromethyl)pyrazol-4-yl]-2-pyridyl]methanamine **5c** (80 mg, 0.30 mmol, 1 eq) was added, and the mixture was stirred at room temperature for 2 h. The mixture was diluted (DCM), washed (saturated NH_4Cl and saturated $NaHCO_3$), dried (filtered through phase separator), and concentrated. The residue was purified by preparatory HPLC (gradient from 40% MeCN to 65% MeCN in water/0.1% formic acid) to afford the desired product (14 mg, 20% yield). LCMS: method B, R_t: 1.36 min; purity: >99%, m/z = 469.2 $(M + H)^+$. ^1H NMR (400 MHz, DMSO-d_6) δ 9.49 (s, 1H), 8.25 (s, 1H), 8.07 (s, 1H), 7.29 (s, 1H), 7.18−7.10 (m, 2H), 6.78 (d, J = 1.5 Hz, 1H), 4.41 (d, J = 5.5 Hz, 2H), 4.21 (q, J = 7.0 Hz, 2H), 3.99 (s, 3H), 2.16 (s, 3H), 1.28 (t, J = 7.0 Hz, 3H). ^{13}C NMR (101 MHz, DMSO-d_6) δ 164.2, 158.3, 154.8, 152.0, 149.8, 148.1, 147.0, 138.3 (d, J = 35.2 Hz), 134.1, 125.5, 122.5, 126.8−118.0 (m), 116.0, 105.8, 95.7, 62.3, 44.6, 39.9, 19.8, 14.9.

*1-(2-Chloro-6-ethoxy-4-pyridyl)-3-[[5-(1,3-dimethylpyrazol-4-yl)-4-methyl-2-pyridyl]methyl]urea (**32**).* This compound was prepared from **4c** according to the general procedure used for the preparation of **34**. LCMS: method B, R_t: 1.23 min; purity: >99%, m/z = 415.2 $(M + H)^+$. ^1H NMR (400 MHz, DMSO-d_6) δ 9.46 (s, 1H), 8.26 (s, 1H), 7.75 (s, 1H), 7.25 (s, 1H), 7.13 (s, 2H), 6.78 (s, 1H), 4.39 (d, J = 5.4 Hz, 2H), 4.22 (q, J = 7.0 Hz, 2H), 3.81 (s, 3H), 2.21 (s, 3H), 2.07 (s, 3H), 1.28 (t, J = 7.0 Hz, 3H). ^{13}C NMR (101 MHz, DMSO-d_6) δ 164.2, 156.6, 154.8, 152.0, 149.7, 148.1, 146.2, 145.6, 131.4, 128.0, 122.8, 115.4, 105.8, 95.7, 62.3, 44.6, 38.8, 20.1, 14.9, 12.6.

*tert-Butyl ((5-Bromo-4-methylpyridin-2-yl)methyl)carbamate (**1e**).* $NaBH_4$ (13.5 g, 357 mmol, 7 eq) was added in portions to a mixture of 5-bromo-4-methylpyridine-2-carbonitrile **1c** (10 g, 51 mmol, 1 eq), $NiCl_2{\cdot}6H_2O$ (2.4 g, 10 mmol, 0.2 eq), and Boc_2O (33 g, 6.4 mmol, 5 eq) in MeOH (170 mL) at 0 °C. The reaction mixture was stirred at room temperature for 1 h. A further 50 mg of $NaBH_4$ was added, and the reaction was stirred for 1 h. The reaction mixture was filtered through Celite and concentrated. The residue was taken up in DCM and saturated $NaHCO_3$. The two layers were filtered and separated. The organic layer was dried (filtered through phase separator) and concentrated to afford the desired product (7.5 g, 49% yield). LCMS: m/z = 300.9 $(M + H)^+$.

*(5-Bromo-4-methylpyridin-2-yl)methanamine TFA Salt (**2e**).* A mixture of *tert*-butyl ((5-bromo-4-methylpyridin-2-yl)methyl)-carbamate **1e** (7.5 g, 25 mmol, 1 eq) and TFA (14 mL) in DCM (50 mL) was stirred at 45 °C for 1.5 h. The mixture was concentrated. Toluene (100 mL) was added, and the resulting mixture was concentrated (this operation was done twice) to yield the desired product (4.6 g, 58% yield). LCMS: m/z = 200.9 $(M + H)^+$.

*1-((5-Bromo-4-methylpyridin-2-yl)methyl)-3-(2-ethoxy-6-(trifluoromethyl)pyridin-4-yl)urea (**3e**).* A mixture of 1,1′-carbonyl-di-(1,2,4-triazole) (CDT, 4.14 g, 25.3 mmol, 1.7 eq), 2-ethoxy-6-(trifluoromethyl)pyridin-4-amine **4g** (Supporting Information) (5.21 g, 25.3 mmol, 1.7 eq), and pyridine (5.6 mL, 69 mmol, 4.6 eq) in DCM (115 mL) was stirred at 45 °C for 30 min, and then the content was added to a flask containing (5-bromo-4-methylpyridin-2-yl)-methanamine TFA salt (4.6 g, 14.6 mmol, 1 eq) and DIPEA (16 mL, 92 mmol, 6.3 eq) in THF (15 mL). The reaction was stirred at room temperature for 2 h. The reaction was quenched with H_2O. The resulting mixture was extracted with DCM (3x). The combined organic phase was washed (1 M HCl), dried (filtered through a phase separator), and concentrated to afford the desired product (3.2 g, 51% yield). LCMS: m/z = 435.1 $(M + H)^+$.

*1-((5-Bromo-4-methylpyridin-2-yl)methyl)-5-(tert-butyl)-3-(2-ethoxy-6-(trifluoromethyl)pyridin-4-yl)-1,3,5-triazinan-2-one (**4e**).* A mixture of 1-((5-bromo-4-methylpyridin-2-yl)methyl)-3-(2-ethoxy-6-(trifluoromethyl)pyridin-4-yl)urea **3e** (3.2 g, 7.4 mmol, 1 eq), formaldehyde (37% H_2O, 12 mL, 148 mmol, 20 eq), 4-

https://doi.org/10.1021/acs.jmedchem.1c00138
J. Med. Chem. 2021, 64, 6037−6058

methylmorpholine (16.3 mL, 148 mmol, 20 eq), and *t*-$BuNH_2$ (15.7 mL, 148 mmol, 20 eq) in 1:1 EtOH/H_2O (74 mL) was stirred at 100 °C for 1 h. The mixture was diluted with EtOAc and H_2O. The two phases were separated, and the aqueous layer was further extracted with EtOAc. The combined organic layers were dried (Na_2SO_4) and concentrated. The residue was purified by flash column chromatography (SiO_2, 90:10 to 30:70 petroleum ether/EtOAc) to afford the desired product as a yellow oil (2.5 g, 64% yield). LCMS: m/z = 530.1 $(M + H)^+$.

*1-[[5-[(1,3-Dimethylpyrazol-4-yl)amino]-4-methyl-2-pyridyl]-methyl]-3-[2-ethoxy-6-(trifluoromethyl)-4-pyridyl]urea (**35**).* A mixture of 1-((5-bromo-4-methylpyridin-2-yl)methyl)-5-(*tert*-butyl)-3-(2-ethoxy-6-(trifluoromethyl)pyridin-4-yl)-1,3,5-triazinan-2-one **4e** (55 mg, 0.10 mmol, 1 eq), 1,3-dimethyl-1*H*-pyrazol-4-amine (33 mg, 0.3 mmol, 3 eq), $Pd_2(dba)_3$ (9 mg, 0.01 mmol, 0.1 eq), BINAP (12 mg, 0.02 mmol, 0.2 eq), and NaO*t*Bu (14 mg, 0.15 mmol, 1.5 eq) in dry toluene (0.3 mL) was degassed with N_2. The mixture was stirred at 70 °C overnight. The mixture was diluted with EtOAc and washed with H_2O. The two phases were separated, and the aqueous layer was extracted with EtOAc. The combined organic layers were dried (Na_2SO_4) and concentrated. The residue was taken up in 1:1 1,4-dioxane/6 M NaOH (2 mL). The resulting mixture was stirred at 100 °C overnight. The mixture was partitioned between EtOAc and H_2O. The two phases were separated. The organic phase was dried (Na_2SO_4) and concentrated. The residue was purified by preparatory HPLC (gradient from 20% MeCN to 45% MeCN in water/0.1% formic acid) to afford the desired product (2.2 mg, 5% yield). LCMS: method B, R_t: 1.30 min; purity: >99%, m/z = 464.2 $(M + H)^+$. ^1H NMR (400 MHz, DMSO-d_6) δ 9.64 (s, 1H), 7.54 (d, J = 4.3 Hz, 2H), 7.50 (d, J = 1.6 Hz, 1H), 7.11 (t, J = 5.6 Hz, 1H), 7.04−6.98 (m, 2H), 6.49 (s, 1H), 4.32−4.20 (m, 4H), 3.75 (s, 3H), 2.20 (s, 3H), 1.95 (s, 3H), 1.30 (t, J = 7.0 Hz, 3H).

*6-Chloro-4-methyl-pyridazin-3-ol (**2f**).* 3,6-Dichloro-4-methylpyridazine **1f** (2.97 g, 18.2 mmol, 1 eq) in aqueous 3.3 M NaOH (30 mL) was stirred at reflux temperature for 1 h. Once cooled at room temperature, aqueous 50% acetic acid (10 mL) was added to pH ≈ 6 and the resulting solid filtered and washed with water. Purification by silica chromatography (EtOAc/petroleum ether; 25:75 to 100:0) afforded the desired compound (1 g, 38% yield). LCMS: m/z = 144.9, 146.9 $(M + H)^+$.

*6-Hydroxy-5-methylpyridazine-3-carbonitrile (**3f**).* A mixture of 6-chloro-4-methyl-pyridazin-3-ol **2f** (21.7 g, 150 mmol, 1 eq), $Zn(CN)_2$ (22.9 g, 195 mmol, 1.3 eq), $Pd_2(dba)_3$ (6.87 g, 7.5 mmol, 0.05 eq), and 1,1′-bis(diphenylphosphino)ferrocene (6.64 g, 12 mmol, 0.08 eq) in DMF (150 mL) was degassed under nitrogen and heated at 120 °C for 1 h. The resulting mixture was diluted with DCM and saturated $NaHCO_3$. The aqueous layer was separated and extracted with DCM and DCM/*i*PrOH (4:1), dried (Na_2SO_4), filtered, and concentrated. The residue was triturated with a mixture of petroleum ether/EtOAc (3:1), filtered, washed with petroleum ether, and dried to afford the desired compound (17.4 g, 86% yield). LCMS: m/z = 135.9 $(M + H)^+$.

*6-Chloro-5-methylpyridazine-3-carbonitrile (**4f**).* $POCl_3$ (31 mL, 333 mmol, 3 eq) was added to 6-hydroxy-5-methylpyridazine-3-carbonitrile **3f** (15 g, 111 mmol, 1 eq) in acetonitrile (200 mL), and the resulting mixture was heated at reflux temperature until completion of the reaction (4 h). The cooled mixture was concentrated under reduced pressure, and the residue was diluted in acetonitrile (200 mL). This solution was poured into a stirred mixture of ice-cold DCM and aqueous $NaHCO_3$. Solid $NaHCO_3$ was added in portions to attain a pH of approximately 7. Both layers were separated, and the aqueous layer was extracted with DCM. The combined organic layer was dried (Na_2SO_4), filtered, and concentrated to afford the desired compound (16.5 g, 97% yield). LCMS: m/z = 154.0 $(M + H)^+$.

*5-Methyl-6-(1-methyl-3-(trifluoromethyl)-1H-pyrazol-4-yl)-pyridazine-3-carbonitrile (**5f**).* $Pd(PPh_3)_4$ (7.44 g, 6.64 mmol, 0.1 eq) was added to a degassed suspension of 6-chloro-5-methylpyridazine-3-carbonitrile **4f** (64 mmol, 1.0 eq) and 1-methyl-4-(4,4,5,5-tetramethyl-[1,3,2]dioxaborolan-2-yl)-3-trifluoromethyl-1*H*-pyrazole (12.4 g, 45 mmol, 0.7 eq) in DMF (275 mL). The resulting mixture was stirred at room temperature for 1 h. A 2.5 M aqueous Na_2CO_3 solution (64 mL) was added, and the resulting mixture was stirred at 85 °C until completion. The cooled mixture was filtered on Celite and washed with EtOAc. The organic extract was washed three times with brine, dried (Na_2SO_4), and concentrated. Purification by silica chromatography (column: 120 g silica 25 μm; EtOAc/DCM; 0:100 to 10:90) afforded the desired compound (6.8 g, 40% yield). LCMS: m/z = 268.0 $(M + H)^+$.

*[5-Methyl-6-[1-methyl-3-(trifluoromethyl)pyrazol-4-yl]pyridazin-3-yl]methanamine HCl (**6f**).* Pd (10% on charcoal, 4.25 g, 4 mmol, 0.15 eq) was added to a degassed mixture of 5-methyl-6-(1-methyl-3-trifluoromethyl-1*H*-pyrazol-4-yl)-pyridazine-3-carbonitrile **5f** (7.3 g, 27.3 mmol, 1 eq) and aq. 6 M HCl (10 mL, 60 mmol, 2.2 eq) in methanol (180 mL). The mixture was stirred at room temperature under hydrogen (1 atm) until completion of the reaction. The resulting mixture was filtered on Celite and washed with methanol and acetonitrile, and the filtrate was concentrated under reduced pressure. The residue was triturated with Et_2O to afford the hydrochloride salt of the desired compound (8.0 g, 95% yield). LCMS: m/z = 272.1 $(M + H)^+$.

*[5-Methyl-6-[1-methyl-3-(trifluoromethyl)pyrazol-4-yl]pyridazin-3-yl]methanamine (**7f**).* $NaBH_4$ (462 mg, 12.2 mmol, 5 eq) was added portionwise to a mixture of 5-methyl-6-(1-methyl-3-trifluoromethyl-1*H*-pyrazol-4-yl)-pyridazine-3-carbonitrile **5f** (2.44 mmol, 1 eq), TFA (0.94 mL, 12.2 mmol, 5 eq) and $NiCl_2 \cdot 6H_2O$ (233 mg, 0.98 mmol, 0.4 eq) in MeOH (10 mL) at 0 °C. After 3 h, a further 230 mg of $NaBH_4$ (6.1 mmol, 2.5 eq) was added. The resulting mixture was stirred at room temperature for 3 h. The mixture was filtered over Celite and concentrated under reduced pressure. Purification by SCX resin exchange afforded the desired product as a free base. The product was used as such in the next step. LCMS: m/z = 272.1 $(M + H)^+$.

General Procedure for Preparation of Ureas 37, 42, 43, and 48. *1-(2-Chloro-6-ethoxypyridin-4-yl)-3-[5-methyl-6-(1-methyl-3-trifluoromethyl-1H-pyrazol-4-yl)-pyridazin-3-ylmethyl]urea (**37**).* 1,1′-Carbonyl-di-(1,2,4-triazole) (726 mg, 4.42 mmol, 1.5 eq) was added to a mixture of 2-chloro-6-ethoxypyridin-4-ylamine (356 mg, 2.07 mmol, 0.7 eq) in pyridine (0.71 mL, 8.85 mmol, 3 eq) and DCM (15 mL). The reaction mixture was stirred at 45 °C for 30 min. Once cooled to room temperature, [5-methyl-6-[1-methyl-3-(trifluoromethyl)pyrazol-4-yl]pyridazin-3-yl]methanamine **7f** (800 mg, 2.95 mmol, 1.0 eq) was added and the resulting mixture was stirred at room temperature for 1 h. The mixture was diluted with DCM and washed with saturated aqueous NH_4Cl and saturated aqueous $NaHCO_3$. The organic phase was filtered through a phase separator and concentrated under reduced pressure. The residue was purified by silica chromatography (MeOH/DCM; 0:100 to 4:96) followed by triturated in a mixture of methyl *tert*-butyl ether/petroleum ether to afford the desired compound (650 mg, 65% yield). LCMS: method B, R_t: 1.30 min; purity: >99%, m/z = 470.2 $(M + H)^+$. HRMS: calcd mass for $C_{19}H_{20}ClF_3N_7O_2$ $(M + H)^+$ 470.1314; found 470.1321; difference 1.6 ppm. ^1H NMR (400 MHz, DMSO-d_6) δ 9.47 (s, 1H), 8.29 (s, 1H), 7.56 (d, J = 1.0 Hz, 1H), 7.28 (t, J = 5.6 Hz, 1H), 7.13 (d, J = 1.5 Hz, 1H), 6.78 (d, J = 1.5 Hz, 1H), 4.61 (d, J = 5.6 Hz, 2H), 4.22 (q, J = 7.0 Hz, 2H), 4.02 (s, 3H), 2.26 (d, J = 0.9 Hz, 3H), 1.28 (t, J = 7.0 Hz, 3H). ^{13}C NMR (101 MHz, DMSO-d_6) δ 164.2, 159.4, 154.9, 153.5, 151.9, 148.2, 138.7 (q, J = 36.1 Hz), 137.8, 134.3, 126.6, 126.3−117.3 (m), 116.7, 105.9, 95.8, 62.4, 43.3, 40.2, 19.2, 14.9. mp = 205 °C.

General Procedure for Preparation of Ureas 38−41, 46, 47, and 50−51. *1-(2-Ethoxy-6-trifluoromethylpyridin-4-yl)-3-[5-methyl-6-(1-methyl-3-trifluoromethyl-1H-pyrazol-4-yl)-pyridazin-3-ylmethyl]urea (**40**).* A mixture of 1,1′-carbonyl-di-(1,2,4-triazole) (1.14 g, 6.97 mmol, 1.2 eq) was added to a mixture of 2-ethoxy-6-(trifluoromethyl)pyridin-4-amine **4g** (Supporting Information) (1.44 g, 6.97 mmol, 1.2 eq) in dry pyridine (1.41 mL, 17.4 mmol, 3.0 eq) and dry DCM (29 mL). The resulting mixture was stirred at 45 °C for 30 min. The abovementioned mixture was added to a suspension of [5-methyl-6-[1-methyl-3-(trifluoromethyl)pyrazol-4-yl]pyridazin-3-

https://doi.org/10.1021/acs.jmedchem.1c00138
J. Med. Chem. 2021, 64, 6037−6058

yl]methanamine hydrochloride salt **6f** (2.0 g, 5.81 mmol, 1.0 eq) and diisopropylethylamine (4.0 mL, 4.0 eq) in dry THF (8.0 mL). The resulting mixture was stirred at room temperature for 30 min. The reaction was performed four times with the same amounts. After completion, the reactions were combined. The resulting mixture was diluted with DCM and water. The organic phase was washed with 1 M HCl solution, filtered through a phase separator, and concentrated under reduced pressure. The crudes were gathered and purified by flash chromatography on silica gel (eluting with Et_2O/Acetone 95/5 to 90/10) to give, after trituration in MTBE/MeCN, the desired compound (11.0 g, 94% yield). LCMS: method B, R_t: 1.36 min; purity: >99%, m/z = 504.3 $(M + H)^+$. HRMS: calcd mass for $C_{20}H_{20}F_6N_7O_2$ $(M + H)^+$ 504.1577; found 504.1586; difference 1.7 ppm. ^{1}H NMR (400 MHz, DMSO-d_6) δ 9.68 (s, 1H), 8.29 (s, 1H), 7.57 (s, 1H), 7.52 (d, J = 1.6 Hz, 1H), 7.37 (t, J = 5.5 Hz, 1H), 7.05 (d, J = 1.6 Hz, 1H), 4.62 (d, J = 5.5 Hz, 2H), 4.29 (q, J = 7.0 Hz, 2H), 4.02 (s, 3H), 2.26 (d, J = 0.8 Hz, 3H), 1.31 (t, J = 7.0 Hz, 3H). ^{13}C NMR (101 MHz, DMSO-d_6) δ 165.0, 159.4, 155.0, 153.5, 151.0, 144.8 (q, J = 33.5 Hz), 138.7 (q, J = 36.1 Hz), 137.8, 134.3, 126.6, 126.0−117.7 (m), 126.1−117.6 (m), 116.7, 104.5 (d, J = 3.8 Hz), 99.8, 62.3, 43.3, 39.8, 19.2, 14.8. mp = 205 °C.

1-[2-Chloro-6-(2,2-difluoroethoxy)-4-pyridyl]-3-[[5-methyl-6-[1-methyl-3-(trifluoromethyl)pyrazol-4-yl]pyridazin-3-yl]methyl]urea (**38**). This compound was prepared from **6f** and **2h** (Supporting Information) according to the general procedure used for the preparation of **40**. LCMS: method B, R_t: 1.32 min; purity: >99%, m/z = 506.3 $(M + H)^+$. HRMS: calcd mass for $C_{19}H_{18}ClF_5N_7O_2$ $(M + H)^+$ 506.1125; found 506.1134; difference 1.7 ppm. ^{1}H NMR (400 MHz, DMSO-d_6) δ 9.57 (s, 1H), 8.29 (s, 1H), 7.57 (d, J = 0.9 Hz, 1H), 7.35 (t, J = 5.6 Hz, 1H), 7.21 (d, J = 1.5 Hz, 1H), 6.91 (d, J = 1.5 Hz, 1H), 6.35 (tt, J = 54.5, 3.4 Hz, 1H), 4.62 (d, J = 5.6 Hz, 2H), 4.50 (td, J = 15.1, 3.4 Hz, 2H), 4.02 (s, 3H), 2.26 (d, J = 0.9 Hz, 3H). ^{13}C NMR (101 MHz, DMSO-d_6) δ 162.9, 159.3, 154.9, 153.5, 152.3, 147.9, 138.7 (q, J = 36.1 Hz), 137.8, 134.3, 126.6, 121.9 (q, J = 268.9 Hz), 116.7, 114.4 (t, J = 238.9 Hz), 106.9, 95.9, 64.4 (t, J = 26.6 Hz), 43.3, 40.1, 19.2. mp = 221−222 °C.

1-(2-Cyano-6-ethoxy-4-pyridyl)-3-[[5-methyl-6-[1-methyl-3-(trifluoromethyl)pyrazol-4-yl]pyridazin-3-yl]methyl]urea (**39**). This compound was prepared from **6f** and **2i** (Supporting Information) according to the general procedure used for the preparation of **40**. LCMS: method B, R_t: 1.24 min; purity: >99%, m/z = 461.1 $(M + H)^+$. ^{1}H NMR (400 MHz, DMSO-d_6) δ 9.62 (s, 1H), 8.29 (s, 1H), 7.57 (t, J = 1.5 Hz, 2H), 7.40 (t, J = 5.6 Hz, 1H), 7.13 (d, J = 1.8 Hz, 1H), 4.62 (d, J = 5.6 Hz, 2H), 4.27 (q, J = 7.0 Hz, 2H), 4.02 (s, 3H), 2.26 (d, J = 0.8 Hz, 3H), 1.30 (t, J = 7.0 Hz, 3H).

1-(2-Ethoxy-6-methyl-4-pyridyl)-3-[[5-methyl-6-[1-methyl-3-(trifluoromethyl)pyrazol-4-yl]pyridazin-3-yl]methyl]urea (**41**). This compound was prepared from **6f** and **2l** (Supporting Information) according to the general procedure used for the preparation of **40**. LCMS: method B, R_t: 1.16 min; purity: >99%, m/z = 450.1 $(M + H)^+$. ^{1}H NMR (400 MHz, DMSO-d_6) δ 9.14 (s, 1H), 8.31 (s, 1H), 7.56 (s, 1H), 7.19−7.12 (m, 1H), 6.74 (d, J = 4.3 Hz, 2H), 4.60 (d, J = 5.5 Hz, 2H), 4.22 (q, J = 7.0 Hz, 2H), 4.02 (s, 3H), 2.27 (d, J = 3.2 Hz, 6H), 1.27 (t, J = 7.1 Hz, 3H). ^{13}C NMR (101 MHz, DMSO-d_6) δ 164.2, 159.6, 156.1, 155.2, 153.4, 150.0, 138.7 (d, J = 36.1 Hz), 137.8, 134.3, 126.6, 126.1−117.1 (m), 116.7, 105.9, 94.4, 61.1, 43.2, 39.9, 24.6, 19.2, 15.1.

1-[2-Chloro-6-(2-methoxyethoxy)-4-pyridyl]-3-[[5-methyl-6-[1-methyl-3-(trifluoromethyl)pyrazol-4-yl]pyridazin-3-yl]methyl]urea (**42**). This compound was prepared from **7f** and **3h** (Supporting Information) according to the general procedure used for the preparation of **37**. LCMS: method B, R_t: 1.21 min; purity: >99%, m/z = 500.0 $(M + H)^+$. ^{1}H NMR (400 MHz, DMSO-d_6) δ 9.49 (s, 1H), 8.29 (s, 1H), 7.56 (d, J = 1.0 Hz, 1H), 7.31 (t, J = 5.6 Hz, 1H), 7.15 (d, J = 1.5 Hz, 1H), 6.81 (d, J = 1.6 Hz, 1H), 4.61 (d, J = 5.5 Hz, 2H), 4.33−4.26 (m, 2H), 4.02 (s, 3H), 3.65−3.58 (m, 2H), 3.29 (s, 4H), 2.26 (d, J = 0.8 Hz, 3H).

1-[2-[2-(Dimethylamino)ethoxy]-6-(trifluoromethyl)-4-pyridyl]-3-[[5-methyl-6-[1-methyl-3-(trifluoromethyl)pyrazol-4-yl]-pyridazin-3-yl]methyl]urea (**43**). This compound was prepared from **7f** and **2k** (Supporting Information) according to the general procedure used for the preparation of **37**. LCMS: method B, R_t: 1.31 min; purity: >99%, m/z = 547.3 $(M + H)^+$. ^{1}H NMR (400 MHz, DMSO-d_6) δ 9.75 (s, 1H), 8.31 (s, 1H), 7.57 (s, 1H), 7.51 (s, 1H), 7.43 (t, J = 5.8 Hz, 1H), 7.07 (s, 1H), 4.62 (d, J = 5.5 Hz, 2H), 4.33 (t, J = 5.8 Hz, 2H), 4.02 (s, 3H), 2.59 (t, J = 5.8 Hz, 2H), 2.27 (s, 3H), 2.19 (s, 6H).

1-(6-Chloro-2-ethoxy-3-methyl-4-pyridyl)-3-[[5-methyl-6-[1-methyl-3-(trifluoromethyl)pyrazol-4-yl]pyridazin-3-yl]methyl]urea (**46**). This compound was prepared from **6f** and **3j** (Supporting Information) according to the general procedure used for the preparation of **40**. LCMS: method B, R_t: 1.38 min; purity: >99%, m/z = 484.2 $(M + H)^+$. HRMS: calcd mass for $C_{20}H_{22}ClF_3N_7O_2$ $(M + H)^+$ 484.1470; found 484.1474; difference 0.8 ppm. ^{1}H NMR (400 MHz, DMSO-d_6) δ 8.52 (s, 1H), 8.32 (s, 1H), 7.88 (d, J = 12.8 Hz, 2H), 7.61 (s, 1H), 4.64 (d, J = 5.3 Hz, 2H), 4.25 (q, J = 7.0 Hz, 2H), 4.03 (s, 3H), 2.28 (s, 3H), 2.03 (s, 3H), 1.31 (t, J = 7.1 Hz, 3H).

1-(6-Cyano-2-ethoxy-3-methyl-4-pyridyl)-3-[[5-methyl-6-[1-methyl-3-(trifluoromethyl)pyrazol-4-yl]pyridazin-3-yl]methyl]urea (**47**). This compound was prepared from **6f** and **3m** (Supporting Information) according to the general procedure used for the preparation of **40**. LCMS: method B, R_t: 1.32 min; purity: >99%, m/z = 475.1 $(M + H)^+$. ^{1}H NMR (400 MHz, DMSO-d_6) δ 8.68 (s, 1H), 8.35 (s, 1H), 8.30 (s, 1H), 7.87 (t, J = 5.3 Hz, 1H), 7.61 (s, 1H), 4.65 (d, J = 5.3 Hz, 2H), 4.31 (q, J = 7.0 Hz, 2H), 4.02 (s, 3H), 2.30−2.25 (m, 3H), 2.11 (s, 3H), 1.33 (t, J = 7.0 Hz, 3H).

1-(2-Ethoxy-3,6-dimethyl-4-pyridyl)-3-[[5-methyl-6-[1-methyl-3-(trifluoromethyl)pyrazol-4-yl]pyridazin-3-yl]methyl]urea (**48**). This compound was prepared from **7f** and **2o** (Supporting Information) according to the general procedure used for the preparation of **37**. LCMS: method B, R_t: 1.29 min; purity: >99%, m/z = 464.2 $(M + H)^+$. HRMS: calcd mass for $C_{21}H_{25}F_3N_7O_2$ $(M + H)^+$ 464.2016; found 464.2027; difference 2.3 ppm. ^{1}H NMR (400 MHz, DMSO-d_6) δ 8.30 (d, J = 1.1 Hz, 1H), 8.21 (s, 1H), 7.67 (t, J = 5.5 Hz, 1H), 7.63−7.56 (m, 2H), 4.62 (d, J = 5.4 Hz, 2H), 4.26 (q, J = 7.0 Hz, 2H), 4.02 (s, 3H), 2.30−2.24 (m, 6H), 2.00 (s, 3H), 1.29 (t, J = 7.0 Hz, 3H). ^{13}C NMR (101 MHz, DMSO-d_6) δ 161.4, 159.5, 155.2, 153.4, 152.2, 147.4, 138.7 (q, J = 36.0 Hz), 137.8, 134.3, 126.8, 121.9 (q, J = 269.2 Hz), 116.7, 106.9, 102.1, 61.3, 43.3, 39.9, 24.6, 19.2, 15.2, 9.6. mp = 195−196 °C.

1-(3-Chloro-2-ethoxy-6-methyl-4-pyridyl)-3-[[5-methyl-6-[1-methyl-3-(trifluoromethyl)pyrazol-4-yl]pyridazin-3-yl]methyl]urea (**50**). This compound was prepared from **6f** and **1n** (Supporting Information) according to the general procedure used for the preparation of **40**. LCMS: method A, R_t: 1.38 min; purity: >99%, m/z = 484.1 $(M + H)^+$. HRMS: calcd mass for $C_{20}H_{22}ClF_3N_7O_2$ $(M + H)^+$ 484.1470; found 484.1479; difference 1.8 ppm. ^{1}H NMR (400 MHz, DMSO-d_6) δ 8.62 (s, 1H), 8.30 (d, J = 1.1 Hz, 1H), 8.15 (t, J = 5.5 Hz, 1H), 7.81 (s, 1H), 7.59 (d, J = 0.9 Hz, 1H), 4.63 (d, J = 5.5 Hz, 2H), 4.34 (q, J = 7.1 Hz, 2H), 4.02 (s, 3H), 2.30 (d, J = 0.6 Hz, 3H), 2.27 (d, J = 0.9 Hz, 3H), 1.32 (t, J = 7.0 Hz, 3H).

1-(3-Cyano-2-ethoxy-6-methyl-4-pyridyl)-3-[[5-methyl-6-[1-methyl-3-(trifluoromethyl)pyrazol-4-yl]pyridazin-3-yl]methyl]urea (**51**). This compound was prepared from **6f** and **1q** (Supporting Information) according to the general procedure used for the preparation of **40**. LCMS: method B, R_t: 1.22 min; purity: >99%, m/z = 475.2 $(M + H)^+$. ^{1}H NMR (400 MHz, DMSO-d_6) δ 11.16 (s, 1H), 9.04 (s, 1H), 8.26 (s, 1H), 7.47 (s, 1H), 6.53 (s, 1H), 5.43 (s, 2H), 4.46 (q, J = 7.1 Hz, 2H), 4.01 (s, 3H), 2.35 (s, 3H), 2.21 (s, 3H), 1.38 (t, J = 7.0 Hz, 3H).

Calcium Flux Assay. The compounds were assessed for they potential agonist activity and, in the same round, for their potential antagonist effect.

Agonist Assay. CHO cells stably overexpressing human GPCR sphingosine 1-phosphate receptor 2 were seeded in 384-well sterile microplates (50 μL; 7500 cells/well) and were incubated overnight at 37 °C under 5% CO_2. Cells were subsequently washed twice with 25 μL/well of starvation medium (F-12 Ham's medium containing 0.1% BSA (FAF)) then starved for 1 h at 37 °C, 5% CO_2 and loaded with 25 μL of Fluo 8 dye diluted in HBSS buffer plus 20 mM HEPES following the recommendations of the manufacturer (Tebu-bio) complemented with 5 mM probenecid. The cells were incubated for 1

https://doi.org/10.1021/acs.jmedchem.1c00138
J. Med. Chem. 2021, 64, 6037−6058

h at 37 °C under 5% CO_2. Dilution series of compounds were diluted in HBSS buffer plus 20 mM HEPES plus 0.1% BSA (FAF). Ten microliters of the diluted compound was added to the cells using the FDSS/μCELL, and intracellular calcium changes were immediately measured by reading the fluorescence for 3 min. The ratio of maximal signal over background before compound injection was used to determine compound response.

Antagonist Assay. After readout of the agonist activity, the plates were incubated 15 min at 37 °C. Then, the plates were transferred to the FDSS/μCELL reader and cells were stimulated with 10 μL of EC_{80} concentration of sphingosine 1-phosphate. Intracellular calcium changes were immediately measured by reading the fluorescence for 3 min. The ratio of maximal signal over background before compound injection was used to determine the compound response. For EC_{50}/IC_{50} determination, a 10-point dilution series of compounds starting from 23.3 μM and 20 μM highest final concentration for agonist and antagonist, respectively, 1/3 dilution was performed. The obtained ratios for agonist and antagonist readout were normalized versus vehicle and EC_{100} of S1P as controls for agonist mode and versus vehicle and EC_{80} of S1P for antagonist mode. From these normalized data, EC_{50} and IC_{50} of the compounds were derived.

GTPγS Assay. The [^{35}S] GTPγS assay measures the level of G protein activation following agonist occupation of a GPCR by determining the binding of the non-hydrolyzable analog [^{35}S] GTPγS to Gα subunits. Compounds (serial dilutions, 96-well LIA plate) and S1P at EC_{80} concentration were incubated with a mixture consisting of membranes derived from stable cell lines overexpressing recombinant human S1P2, [^{35}S]GTPγS, and SpA beads (Perkin Elmer, RPNQ0001). Reactions (50 μL cpd + 30 μL S1P2 membrane preincubated with PVT-WGA SPA beads +20 μL S1P at EC_{80}) were incubated at room temperature for 4 h followed by centrifugation (20 min, 2000 rpm). Plates were read on a TopCount reader (Molecular Devices, ^{35}S-GTPγS, 1 min readout time/well) immediately after centrifugation.

Radioligand-Based Binding Assay. The following assay can be used for determination of S1PR2 binding. The binding assay measures the potential to compete with radioactively labeled S1P for binding to the receptor. The assay was performed in a 96-well plate where the following reagents are added (final concentrations: 1% DMSO, 7.5 nM radiolabeled S1P, 20 μM to 1 nM 1/3 serial dilutions of test compounds). First, 50 μL of compound solution (serial dilution; 4% DMSO/buffer) is added into the assay plate followed by addition of 100 μL of a mixture consisting of membrane and scintillation proximity assay (SpA) beads [mixture consists of 20 μg/well membranes derived from stable cell lines overexpressing S1PR2, 0.5 mg/well polyvinyltoluene-wheat germ-agglutinin (PVT-WGA) beads (Perkin Elmer, RPNQ0001)]. All components were diluted in assay buffer containing 20 mM Tris pH 7.5; 10 mM $MgCl_2$; 100 mM NaCl; 0.4% BSA FAF; 1 mM Na_3VO_4) and incubated for 15 min until addition to the assay plate. Subsequently, 50 μL of radioactively labeled S1P (7.5 nM final concentration) was added to the wells (Sphingosine, D-erythro-[3-^{3}H] 1-phosphate; ARC; ART0778). After incubation for 2 h at room temperature, plates were centrifuged at 2000 rpm for 20 min. Plates were read on a TopCount reader (Perkin Elmer) immediately after centrifugation (readout time, 1 min/well).

IL8 Assay (in the Absence and Presence of 2% HSA). The assay was performed in two formats, 96 and 384 wells. The values from the two formats were in good agreement. For the compounds tested in both assays, IC_{50} values are reported as geometrical means. For compounds tested only in one of the two assays, IC_{50} values are reported without distinction. Two conditions were applied: with and without 2% human serum albumin (HSA, equivalent to approximately 40% serum).

Seven days before seeding, HFL-1 cells were thawed in growth/seeding medium (F12K medium complemented with 10% heat-inactivated FBS and 1% Pen/strep) and incubated at 37 °C, 5% CO_2. Three days before seeding, the cells were split once. Forty (6000 cells/well) or 100 μL (16,000 cells/well) HFL-1 cells were seeded in growth/seeding medium in 384-well or 96-well plates, respectively. Plates were incubated at room temperature for 1 h followed by overnight incubation at 37 °C, 5% CO_2. The medium was replaced with 64 μL (384 well) or 160 μL (96 well) starvation medium containing 1% heat-inactivated FBS, 1% P/S with or without 1.95% HSA (corresponding to approximately 40% serum) for 16−24 h at 37 °C, 5% CO_2. Eight microliters of a 10-point serial dilution, 30 μM highest final concentration, 1/3 dilution was added to the cells. Plates were incubated for 1 h at 37 °C, 5% CO_2 followed by the addition of 20 μL (96 format)/8 μL (384 format) S1P at EC_{80} concentration (1 μM, 96 format, or 0.5 μM, 384 format, final concentration for plates without HSA; 5 μM, 96 format, or 2 μM, 384 format, final concentration for plates with HSA) to the sample and vehicle wells. No trigger was added to the wells to be used as a positive control. Plates were incubated for 16−24 h at 37 °C, 5% CO_2. ELISA plates were coated with 40 μL of 1 μg/mL IL8 capture antibody and incubated overnight at 4 °C. ELISA plates were blocked using 80 μL of sucrose blocking buffer for 4 h at room temperature. Forty microliters of the supernatant was harvested on the ELISA plates followed by overnight incubation at 4 °C. Thirty-five microliters of 50 ng/mL detection antibody was added to the ELISA plates, which were incubated for 2 h at room temperature. Subsequently, 35 μL (500 ng/mL) Strep-HRP was added followed by 45−60 min incubation in the dark. Lastly, 50 μL of luminol substrate was added and chemiluminescence was read on the Envision after 5 min room temperature incubation in the dark.

Free IC_{50} values were calculated from the following equation:

$$\text{free } IC_{50} = IC_{50} \times \text{fu, medium} \quad (1)$$

where fu, medium was determined from the following equation:

$$\text{fu, medium} = \frac{1}{(\text{protein\%})\left(\frac{1}{\text{fu}} - 1\right) + 1} \quad (2)$$

where fu is the fraction unbound from the hPPB assay and protein% is the percentage of serum used in the assay.

S1P-Induced Collagen Gel Lattice Contraction. Normal human lung fibroblasts (Promocell) were treated with 1 ng/mL TGF-β (Gibco, PHG92I4) for 4 days in FGM-2 culture medium (Lonza, CC3132). 96 h after seeding the cells in medium containing TGF-β, and the cells were harvested and embedded in collagen lattices. Collagen lattices were prepared by mixing 8 parts PureCol (acidic collagen I solution at 3 mg/mL, Advanced Biomatrix, 5005-100 mL) with 1 part 10X medium or DPBS and 1 part HEPES 0.2 M at pH 8.0 (to neutralize the pH of the collagen solution and the stiffening of the gel), and cells were added in a 1 part/volume of the collagen gel at a cell density of 200,000 cells per gel. Per well of a 24 well plate (Greiner Bio-one, 662160), 550 μL of collagen gel with cells was used, consisting of 400 μL of PureCol, 50 μL of 10X PBS, and 50 μL of HEPES 0.2 M at pH 8.0 together with 50 μL of cell suspension. Plates were incubated for 1.5−2 h at 37 °C 5% CO_2. After 2 h of gel formation, 1 mL of FGM without serum supplemented with 1 ng/mL TGF-β was added to the collagen gel. The plates were incubated for 72 h at 37 °C 5% CO_2 for stress build-up. Seventy-two hours after collagen gel formation, the gels were treated with compounds diluted in FGM-2 serum free medium. Two hours after compound incubation, 1 μM S1P (Avanti Polar lipids, 860,492) was added and the treated gels were released from the sides of the wells after which the plates were incubated at 37 °C 5% CO_2 for another hour. Images were taken at the end of the assay and analyzed with ImageJ software.

Liver Microsomal Stability Assay. A 10 mM stock solution of compound in DMSO was diluted three-fold in DMSO. This pre-diluted compound solution was then diluted to 2 μM in a 100 mM phosphate buffer (pH 7.4) and pre-warmed at 37 °C. This compound dilution was mixed 1/2 with a microsomal/cofactor mix at 37 °C under shaking at 300 rpm. Final reaction conditions are as follows: 100 pL incubation volume, 1 μM test compound (n = 2), 0.2% DMSO, 0.5 mg/mL microsomes (Xeno-Tech, Kansas City, KS, USA), 0.6 U/mL glucose-6-phosphate-dehydrogenase (G6PDH, Roche, 10127671001), 3.3 mM mgCb (Sigma, M2670), 3.3 mM glucose-6-phosphate (Sigma, G-7879), and 1.3 mM NADP+ (Sigma, N-0505).

https://doi.org/10.1021/acs.jmedchem.1c00138
J. Med. Chem. 2021, 64, 6037−6058

After 30 min of incubation at 300 rpm and 37 °C, the reaction was stopped with 600 μL of STOP solution (Acetonitrile with Diclofenac as internal standard). For the zero-time point, 600 μL of STOP solution were added to the compound dilution before the microsome mix was added. The samples of both time points were centrifuged and filtered, and the supernatant analyzed by LC-MS/MS. The samples were analyzed on LC/MS-MS with a flow rate of 0.6 mL/min. The mobile phase A was 0.1% formic acid in H_2O, and the mobile phase B was 0.1% formic acid in 90% MeCN and 10% H_2O. The sample was run under positive or negative ion spray on Pursuit C18, 5 pm (2.0 x 20 mm) column, from Agilent. The instrument responses (peak areas/IS peak area) were referenced to the zero time-point samples (considered as 100%) in order to determine the percentage of compound remaining. Verapamil (1 μM) and warfarin (1 μM) were used as reference compounds, as unstable and stable compounds, respectively. If the microsomal stability values for these controls are not in the range determined by the historical data, the assay is not validated. The data on microsomal stability are expressed as a percentage of the total amount of compound remaining after 30 min incubation. The solubility of the compound in the final test concentration in 100 mM buffer pH 7.4 was checked using a microscope to indicate whether precipitation occurred. For the calculation of the half-life, a first-order kinetic was assumed. Intrinsic clearance (Clint) and scaled intrinsic clearance (scaled Clint) values were obtained with the equations below:

Intrinsic clearance equation:

$$\text{Clint}[\mu\text{L mg}^{-1}\text{ min}^{-1}] = \frac{\ln 2}{t_{1/2}[\text{min}]} \times \frac{\text{incubation volume}[\mu\text{L}]}{\text{mg of protein}} \quad (3)$$

Scaled intrinsic clearance equation:

$$\text{scaled Clint}[\text{L h}^{-1}\text{kg}^{-1}] = \text{Clint}[\mu\text{L mg}^{-1}\text{ min}^{-1}] \times \frac{\text{microsomal protein (mg)}}{\text{g of liver}} \times \frac{\text{liver weight(g)}}{\text{body weight(kg)}} \times \frac{60}{1000000} \quad (4)$$

To take into account nonspecific binding, scaled Clint values were corrected with the fraction unbound in microsomes (fu, mic),[44] according to the equation below:

Scaled intrinsic clearance unbound (clearance unbound) equation:

$$\text{Clint, u}[\text{L h}^{-1}\text{kg}^{-1}] = \frac{\text{scaled Clint}[\text{L h}^{-1}\text{kg}^{-1}]}{\text{fu, mic}} \quad (5)$$

Fu, mic values were experimentally determined. In case it was not possible, the values were calculated using a global Random Forest regression model.[45]

Fu, mic Determination. Equilibrium dialysis is a technique used to measure microsomal binding. Briefly, the assay was performed in a 96-well Teflon dialysis unit (Dialysis Device, model HTD96b), where each well consists of two chambers separated by a dialysis membrane (membrane strips, MW cutoff 12−14 kDa, HTDialysis). Inactivated liver microsomes (pooled human liver microsomes, Xenotech, protein concentration of 0.5 mg/mL) spiked with a compound (1 μM final concentration, 0.5% DMSO) were added to one chamber and buffer solution (50 mM PBS Buffer) to the other side of the well. Each compound was analyzed in duplicate, for 4 h at 37 °C. At the end of incubation, both chambers were sampled and analyzed by LC-MS/MS. The unbound microsomal fraction (fu, mic) was calculated as the concentration in buffer divided by the total concentration in the microsomal side. Positive controls included in this assay are terfenadine and verapamil.

PK Mouse. These studies were performed with naïve male CD1 mice (Janvier France, 4−5 weeks old). Mice were dosed iv via a bolus in the tail vein with a dose level of 1 mg/kg or orally as a single oesophageal gavage with a dose level of 5 mg/kg. For the iv route, the compound was formulated in PEG 200/water (60/40; v/v). For the oral route, the compound was formulated in Tween 80/MC 0.5% or PEG400/MC 0.5%. Before the oral dosing, the animals were deprived of food for at least 12 h before compound administration and 3 h after administration. All animals had free access to tap water. Blood samples were collected under light anesthesia and placed into tubes containing Li-heparin as an anticoagulant. Blood samples were collected up to 24 h after dosing (composite design: n = 6 mice per route, 2 groups of 3 mice sampled at alternate time points). After centrifugation, the resulting plasma samples were assayed by LC-MS/MS with a non-good-laboratory-practice (non-GLP)-validated method. PK parameters were calculated by noncompartmental analysis using WinNonlin software (Certara, Princeton, NJ, USA).

PK Rat. These studies were performed with naïve male Sprague Dawley rats (Janvier France, 6−8 weeks old). Rats were dosed iv via a bolus in the tail vein with a dose level of 1 mg/kg or orally as a single oesophageal gavage with a dose level of 5 mg/kg (10 mg/kg for compound **48**). For the iv route, the compound was formulated in PEG200/water (60/40; v/v). For the oral route, the compound was formulated in PEG400/MC 0.5%. Before the oral dosing, the animals were deprived of food for at least 12 h before compound administration and 3 h after administration. All animals had free access to tap water. Blood samples were collected under light anesthesia and placed into tubes containing Li-heparin as an anticoagulant. Blood samples were collected up to 24 h after dosing (n = 3 rats per route, n = 2 for the iv PK study of compound **40**). After centrifugation, the resulting plasma samples were assayed by LC-MS/MS with a non-good-laboratory-practice (non-GLP)-validated method. PK parameters were calculated by noncompartmental analysis using WinNonlin software (Certara, Princeton, NJ, USA).

PK Dog. These studies were performed with non-naïve male Beagle dogs (compound **37**: age 13.8 months old, origin: Marshall US, North Rose, NY 14516, USA; compound **40**: age 15.8 months old, origin: Harlan; compound **48**: age 17.7 months old, origin: Harlan). Dogs (n = 3) were dosed iv via a 10 min infusion via a catheter with a dose level of 1 mg/kg. After a washout of 3 days, they were dosed orally as a single gavage with a dose level of 5 mg/kg or 1 mg/kg in PEG400/MC 0.5% or MC 0.5%. Before administration by the po route, animals were fasted for a period of at least 12 h before treatment, and food was given just after the 3 h blood sampling. All animals had free access to tap water. Blood samples were taken without an anesthetic from a jugular or cephalic vein into tubes containing lithium heparin as an anticoagulant. Blood samples were taken up to 24 h after the start of infusion. After centrifugation, the resulting plasma samples were assayed by LC-MS/MS with a non-good-laboratory-practice (non-GLP)-validated method. PK parameters were calculated by noncompartmental analysis using WinNonlin software (Certara, Princeton, NJ, USA).

Prophylactic Bleomycin-Induced Pulmonary Fibrosis 14-day Mice Model. The aim of these studies is to test the efficacy of test compounds in a 14-day model of bleomycin-induced pulmonary fibrosis in mice. The studies were performed at Fidelta Ltd., Zagreb, Croatia.

Animals. These studies were carried out on C57BL/6 N male mice, supplied by Charles River, Italy, which are acclimatized for 7 days after arrival in an environment maintained at 22 °C, at 55% relative humidity, with 15−20 air changes per hour under light cycles of 12 h. Mice were 8 weeks old on arrival for the study involving compound **40** and 7 weeks old on arrival for the study with compound **48**. Mice pelleted food and water are provided ad libitum. At least 1 day prior to the start of experiment, all animals were allocated randomly into groups of 15 (study with compound **40**) or 14 (study with compound **48**). All animal related research is conducted in accordance with the 2010/63/EU and National legislation regulating the use of laboratory animals in scientific research and for other purposes (Official Gazette 55/13).

Materials. The solvent for the test solutions was prepared by adding 0.5 g of hydroxyethyl cellulose (Natrosol) into 500 mL of aqua distillate (0.1%) under continuous stirring without heating for 5 h on a magnetic stirrer. Anesthetic solution was prepared by adding 1 mL of Narketan (Narketan 10, Vetoquinol, Bern, Switzerland,

https://doi.org/10.1021/acs.jmedchem.1c00138
J. Med. Chem. 2021, 64, 6037−6058

03605877535982) and 0.5 mL of Rompun (Rompun, 2%: Bayer, Leverkusen, Germany) into 9 mL of saline. The resulting solution was administered at 10 mL/kg. To prepare a solution for intranasal challenge (i.n.) challenge, 0.8 mg/mL stock solutions of bleomycin (bleomycin sulfate, Enzo Life Sciences, Inc., USA; CAS no. 9041-93-4; cat. no. BML-AP302-0010) were thawed and diluted in 330 μL of saline. Prior to i.n. administration, mice were anesthetized i.p. with the anesthetic solution described above. Fresh pirfenidone formulation was prepared daily in 0.1% Natrosol formulations to a final concentration of 5 mg/mL. Before dosing, animals were weighed and the pirfenidone amount administered was adjusted accordingly to individual weights corresponding to 10 mL/kg body weight, twice daily p.o., with 7.5 h interval between two administrations. Finally, test compound solutions were prepared by dissolving a suitable amount of the test compound in PEG 400 (20% of the final volume) then MC 0.5% (80% of the final volume) to reach final concentrations of 1, 0.3, and 0.1 mg/mL, thus yielding compounds for doses of 10, 3, and 1 mg/kg (compound **40**) or in an exact volume of MC 0.5% to reach a final concentration of 0.3, 1, and 3 mg/mL for doses of 3, 10, and 30 mg/kg (compound **48**). Prior to dosing, animals were weighed, and the amount administered was adjusted accordingly to individual weights. The application volume of the test doses corresponds to 10 mL/kg body weight, and the test compounds were administered p.o. twice daily, with 7.5 h interval between two administrations.

Study. Animals were examined clinically twice daily. Animals were weighed daily starting from day 0. On day 14, 2 h post-dosing with pirfenidone or the test compound, mice were sacrificed by anesthetic overdose. The lungs were excised and weighed individually. For all groups, the whole superior right lung lobe was placed into a Precellys tube containing silica beads and immediately snap frozen in liquid nitrogen and subjected to gene expression analysis. All remaining lungs were placed into marked bottles containing 10% buffered formalin for further histopathological evaluation. For the study involving compound **40**, two satellite groups were used (n = 6 per groups) to assess the ssPK for the 3 and 10 mg/kg doses, respectively. These animals were treated with bleomycin and the test compound exactly as the other animals in the study. They were sacrificed at day 7. A minimal target volume of 50 μL of blood was collected into Li-heparin anticoagulant tubes for each time point. The tubes were kept on ice until separation. Within maximum 30 min after collection, blood samples were centrifuged at 2000g for 10 min at 4 °C and the resulting plasma samples were aliquoted into polypropylene tubes (1 x 25 μL). Samples were stored frozen at −20 °C until analysis. Blood samples were collected from the tail vein. Lung tissue was collected at sacrifice, after blood sampling for each animal, weighed, placed into tubes, and stored frozen at −80 °C until analysis.

Sample Analysis, Data Processing, and Statistical Evaluation. For histopathological evaluation, whole lungs (except sampled superior right lung) were embedded in paraffin and stained with Mallory's trichrome. Pulmonary histological changes were assessed using Matsuse modification of Ashcroft score.[40,41] Statistical analysis and graphical presentation were performed using GraphPad Prism software (version 5.04). The Mann−Whitney test was employed. Differences between groups will be considered statistically significant when $p < 0.05$. For the ssPK study, after centrifugation, the resulting plasma samples were assayed by LC-MS/MS with a non-good-laboratory-practice (non-GLP)-validated method. Lung samples were homogenized and then processed as the plasma samples. PK parameters of compound **40** were calculated by noncompartmental analysis using WinNonlin software (Certara, Princeton, NJ, USA).

All animal experiments performed in the manuscript were conducted in compliance with institutional guidelines.

■ ASSOCIATED CONTENT

Supporting Information

The Supporting Information is available free of charge at https://pubs.acs.org/doi/10.1021/acs.jmedchem.1c00138.

Activity of **40** against S1P receptors; activity of **48** against S1P receptors; DR of **40** against receptors and enzymes from a Cerep broad selectivity panel; steady state PK and IC_{50} coverage of compound **40** (IL8 assay) in BLM-induced pulmonary fibrosis model; synthesis of 4-aminopyridines intermediates for the synthesis of final compounds **38**−**51**; synthesis of final compounds **44**, **45**, and **49**; synthesis of final compounds **36**, **52**−**57**, **97**, **98**, and **101**; detailed SAR of investigation of the C5 position of pyridine series; synthesis of final compounds **65**, **72**, and **120**−**124**; recombinant CYP inhibition of compounds **34**, **37**, and **40**; CYP HLM inhibition of compound **40**; chemical stability at different pH values and plasma stability of compound **40**; hERG inhibition of compound **40**; LCMS analyses of compounds **34**, **40**, and **48** and HRMS spectra of **40** and **48**; SAR of compounds **52**−**57** (from Figure 5 of the main text); and IC_{50} values in S1P2 calcium flux assay (all runs) for compounds **19** and **20** (PDF)

Molecular formula strings (CSV)

■ AUTHOR INFORMATION

Corresponding Authors

Oscar Mammoliti − *Galapagos NV, 2800 Mechelen, Belgium;* orcid.org/0000-0002-1521-9254; Phone: +32 15 34 29 00; Email: oscar.mammoliti@glpg.com

Adeline Palisse − *Galapagos NV, 2800 Mechelen, Belgium;* Phone: +32 15 34 29 00; Email: adeline.palisse@glpg.com

Authors

Caroline Joannesse − *Galapagos NV, 2800 Mechelen, Belgium*

Sandy El Bkassiny − *Galapagos NV, 2800 Mechelen, Belgium*

Brigitte Allart − *Galapagos NV, 2800 Mechelen, Belgium*

Alex Jaunet − *Galapagos NV, 2800 Mechelen, Belgium*

Christel Menet − *Galapagos NV, 2800 Mechelen, Belgium*

Beatrice Coornaert − *Galapagos NV, 2800 Mechelen, Belgium*

Kathleen Sonck − *Galapagos NV, 2800 Mechelen, Belgium*

Inge Duys − *Galapagos NV, 2800 Mechelen, Belgium*

Philippe Clément-Lacroix − *Galapagos SASU, 93230 Romainville, France*

Line Oste − *Galapagos NV, 2800 Mechelen, Belgium*

Monica Borgonovi − *Galapagos SASU, 93230 Romainville, France*

Emanuelle Wakselman − *Galapagos SASU, 93230 Romainville, France*

Thierry Christophe − *Galapagos NV, 2800 Mechelen, Belgium*

Nicolas Houvenaghel − *Galapagos NV, 2800 Mechelen, Belgium*

Mia Jans − *Galapagos NV, 2800 Mechelen, Belgium*

Bertrand Heckmann − *Galapagos SASU, 93230 Romainville, France*

Laurent Sanière − *Galapagos SASU, 93230 Romainville, France*

Reginald Brys − *Galapagos NV, 2800 Mechelen, Belgium*

Complete contact information is available at: https://pubs.acs.org/10.1021/acs.jmedchem.1c00138

Notes

The authors declare no competing financial interest.

■ ACKNOWLEDGMENTS

We are grateful to Stella Adriaens and Tiny Deschrijver for the work performed in the HPLC purification of the final compounds. We thank Marie-Pierre Delage for performing the HRMS spectra and Pieter Stouten for the description of the model used for the fu, mic calculations.

■ REFERENCES

(1) (a) Fyrst, H.; Saba, J. D. An update on sphingosine-1-phosphate and other sphingolipid mediators. *Nat. Chem. Biol.* **2010**, *6*, 489−497. (b) Strub, G. M.; Maceyka, M.; Hait, N. C.; Milstien, S.; Spiegel, S. Extracellular and intracellular actions of sphingosine-1-phosphate. *Adv. Exp. Med. Biol.* **2010**, *688*, 141−155. (c) Blaho, V. A.; Hla, T. An update on the biology of sphingosine 1-phosphate receptors. *J. Lipid Res.* **2014**, *55*, 1596−1608. (d) Spiegel, S.; Milstien, S. Sphingosine-1-phosphate: an enigmatic signalling lipid. *Nat. Rev. Mol. Cell Biol.* **2003**, *4*, 397−407. (e) Brinkmann, V. Sphingosine 1-phosphate receptors in health and disease: mechanistic insights from gene deletion studies and reverse pharmacology. *Pharmacol. Ther.* **2007**, *115*, 84−105. (f) Mutoh, T.; Rivera, R.; Chun, J. Insights into the pharmacological relevance of lysophospholipid receptors. *Br. J. Pharmacol.* **2012**, *165*, 829−844.

(2) Stepanovska, B.; Huwiler, A. Targeting the S1P receptor signaling pathways as a promising approach for treatment of autoimmune and inflammatory diseases. *Pharmacol. Res.* **2020**, *154*, 104170.

(3) Demont, E. H.; Bailey, J. M.; Bit, R. A.; Brown, J. A.; Campbell, C. A.; Deeks, N.; Dowell, S. J.; Eldred, C.; Gaskin, P.; Gray, J. R. J.; Haynes, A.; Hirst, D. J.; Holmes, D. S.; Kumar, U.; Morse, M. A.; Osborne, G. J.; Renaux, J. F.; Seal, G. A. L.; Smethurst, C. A.; Taylor, S.; Watson, R.; Willis, R.; Witherington, J. Discovery of tetrahydropyrazolopyridine as sphingosine 1-phosphate receptor 3 (S1P3)-sparing S1P1 agonists active at low oral doses. *J. Med. Chem.* **2016**, *59*, 1003−1020. and references therein.

(4) Brinkmann, V.; Billich, A.; Baumruker, T.; Heining, P.; Schmouder, R.; Francis, G.; Aradhye, S.; Burtin, P. Fingolimod (FTY720): Discovery and development of an oral drug to treat multiple sclerosis. *Nat. Rev. Drug Discovery* **2010**, *9*, 883−897.

(5) *NDA 02257-FDA Approved Labeling Text for Gilenya (Fingolimod) Capsules*. Sep 21, 2010, www.accessdata.fda.gov/drugsatfda_docs/label/2010/022527s000lbl.pdf (accessed Dec 15, 2020).

(6) Shea, B. S.; Brooks, S. F.; Fontaine, B. A.; Chun, J.; Luster, A. D.; Tager, A. M. Prolonged exposure to sphingosine 1-phosphate receptor-1 agonists exacerbates vascular leak, fibrosis, and mortality after lung injury. *Am. J. Respir. Cell Mol. Biol.* **2010**, *43*, 662−673.

(7) (a) Gellings Lowe, N.; Swaney, J. S.; Moreno, K. M.; Sabbadini, R. A. Sphingosine-1-phosphate and sphingosine kinase are critical for transforming growth factor-β-stimulated collagen production by cardiac fibroblasts. *Cardiovasc. Res.* **2009**, *82*, 303−312. (b) Keller, C. D.; Gil, P. R.; Tölle, M.; van der Giet, M.; Chun, J.; Radeke, H. H.; Schäfer Korting, M.; Kleuser, B. Immunomodulator FTY720 induces myofibroblast differentiation via the lysophospholipid receptor S1P3 and Smad3 *signaling*. *Am. J. Pathol.* **2007**, *170*, 281−292. (c) Urata, Y.; Nishimura, Y.; Hirase, T.; Yokoyama, M. Sphingosine 1-phosphate induces α-smooth muscle actin expression in lung fibroblasts via Rho-kinase. *Kobe J. Med. Sci.* **2005**, *51*, 17−27.

(8) Sobel, K.; Menyhart, K.; Killer, N.; Renault, B.; Bauer, Y.; Studer, R.; Steiner, B.; Bolli, M. H.; Nayler, O.; Gatfield, J. Sphingosine 1-phosphate (s1p) receptor agonists mediate pro-fibrotic responses in normal human lung fibroblasts via S1P2 and S1P3 receptors and smad-independent signalling. *J. Biol. Chem.* **2013**, *288*, 14839−14851.

(9) Mandala, S.; Hajdu, R.; Bergstrom, J.; Quackenbush, E.; Xie, J.; Milligan, J.; Thornton, R.; Shei, G. J.; Card, D.; Keohane, C.; Rosenbach, M.; Hale, J.; Lynch, C. L.; Rupprecht, K.; Parsons, W.; Rosen, H. Alteration of lymphocyte trafficking by sphingosine-1-phosphate receptor agonists. *Science* **2002**, *296*, 346−349.

(10) Sobel, K.; Monnier, L.; Menyhart, K.; Bolinger, M.; Studer, R.; Nayler, O.; Gatfield, J. FTY720 Phosphate activates sphingosine-1-phosphate receptor 2 and selectively couples to Gα12/13/rho/rock to induce myofibroblast contraction. *Mol. Pharmacol.* **2015**, *87*, 916−927.

(11) (a) Serriere-Lanneau, V.; Teixeira-Clerc, F.; Li, L.; Schippers, M.; de Wries, W.; Julien, B.; Tran-Van-Nhieu, J.; Manin, S.; Poelstra, K.; Chun, J.; Carpentier, S. The sphingosine 1-phosphate receptor S1P2 triggers hepatic wound healing. *FASEB J.* **2007**, *21*, 2005−2013. (b) Takuwa, Y.; Ikeda, H.; Okamoto, Y.; Takuwa, N.; Yoshioka, K. Sphingosine-1-phosphate as a mediator involved in development of fibrotic diseases. *Biochim. Biophys. Acta* **2013**, *1831*, 185−192. (c) Blankenbach, K. V.; Schwalm, S.; Pfeilschifter, J.; Meyer zu Heringdorf, D. Sphingosine-1-phosphate receptor-2 antagonists: therapeutic potential and potential risks. *Front. Pharmacol.* **2016**, *7*, 167. (d) Takuwa, N.; Okamoto, Y.; Yoshioka, K.; Takuwa, Y. Sphingosine-1-phosphate signalling and cardiac fibrosis. *Inflammation Regener.* **2013**, *33*, 096−108. (e) Schwalm, S.; Pfeilschifter, J.; Huwiler, A. Sphingosine-1-phosphate: A Janus-faced mediator of fibrotic diseases. *Biochim. Biophys.* **2013**, *1831*, 239−250. and references therein. (f) Kono, Y.; Nishiuma, T.; Nishimura, Y.; Kotani, Y.; Okada, T.; Nakamura, S.; Yokoyama, M. Sphingosine kinase 1 regulates differentiation of human and mouse lung fibroblasts mediated by TGF-β1. *Am. J. Respir. Cell Mol. Biol.* **2007**, *37*, 395−404. (g) Ikeda, H.; Watanabe, N.; Ishii, I.; Shimosawa, T.; Kume, Y.; Tomiya, T.; Inoue, Y.; Nishikawa, T.; Ohtomo, N.; Tanoue, Y.; Iitsuka, S.; Fujita, R.; Omata, M.; Chun, J.; Yatomi, Y. Sphingosine 1-phosphate regulates regeneration and fibrosis after liver injury via sphingosine 1-phosphate receptor 2. *J. Lipid Res.* **2009**, *50*, 556−564. (h) Milara, J.; Navarro, R.; Juan, G.; Peiró, T.; Serrano, A.; Ramón, M.; Morcillo, E.; Cortijo, J. Sphingosine-1-phosphate is increased in patients with idiopathic pulmonary fibrosis and mediates epithelial to mesenchymal transition. *Thorax* **2012**, *67*, 147−156.

(12) Park, S. J.; Im, D. S. Deficiency of Sphingosine-1-Phosphate Receptor 2 (S1P2) attenuates bleomycin-induced pulmonary fibrosis. *Biomol. Ther.* **2019**, *27*, 318−326.

(13) Zhao, J.; Okamoto, Y.; Asano, Y.; Ishimaru, K.; Aki, S.; Yoshioka, K.; Takuwa, N.; Wada, T.; Inagaki, Y.; Takahashi, C.; Nishiuchi, T.; Takuwa, Y. Sphingosine-1-phosphate receptor-2 facilitates pulmonary fibrosis through potentiating IL-13 pathway in macrophages. *PLoS One* **2018**, *13*, No. e0197604.

(14) Cattoretti, G.; Mandelbaum, J.; Lee, N.; Chaves, A. H.; Mahler, A. M.; Chadburn, A.; Dalla-Favera, R.; Pasqualucci, L.; MacLennan, A. J. Targeted disruption of the S1P2 sphingosine 1-phosphate receptor gene leads to diffuse large B-cell lymphoma formation. *Cancer Res.* **2009**, *69*, 8686−8692.

(15) Muppidi, J. R.; Schmitz, R.; Green, J. A.; Xiao, W.; Larsen, A. B.; Braun, S. E.; An, J.; Xu, Y.; Rosenwald, A.; Ott, G.; Gascoyne, R. D.; Rimsza, L. M.; Campo, E.; Jaffe, E. S.; Delabie, J.; Smeland, E. B.; Braziel, R. M.; Tubbs, R. R.; Cook, J. R.; Weisenburger, D. D.; Chan, W. C.; Vaidehi, N.; Staudt, L. M.; Cyster, J. G. Loss of signalling via Gα13 in germinal centre B-cell-derived lymphoma. *Nature* **2014**, *516*, 254−258.

(16) (a) Kusumi, K.; Shinozaki, K.; Kanaji, T.; Kurata, H.; Naganawa, A.; Otsuki, K.; Matsushita, T.; Sekiguchi, T.; Kakuuchi, A.; Seko, T. Discovery of novel S1P2 antagonists. Part 1: Discovery of 1,3-bis(aryloxy)benzene derivatives. *Bioorg. Med. Chem. Lett.* **2015**, *25*, 1479−1482. (b) Kusumi, K.; Shinozaki, K.; Yamaura, Y.; Hashimoto, A.; Kurata, H.; Naganawa, A.; Ueda, H.; Otsuki, K.; Matsushita, T.; Sekiguchi, T.; Kakuuchi, A.; Seko, T. Discovery of novel S1P2 antagonists. Part 2: Improving the profile of a series of 1,3-bis(aryloxy)benzene derivatives. *Bioorg. Med. Chem. Lett.* **2015**, *25*, 4387−4392. (c) Kusumi, K.; Shinozaki, K.; Yamaura, Y.; Hashimoto, A.; Kurata, H.; Naganawa, A.; Otsuki, K.; Matsushita, T.; Sekiguchi, T.; Kakuuchi, A.; Yamamoto, H.; Seko, T. Discovery of novel S1P2 antagonists. Part 3: Improving the oral bioavailability of a series of 1,3-bis(aryloxy)benzene derivatives. *Bioorg. Med. Chem. Lett.* **2016**, *26*, 1209−1213.

https://doi.org/10.1021/acs.jmedchem.1c00138
J. Med. Chem. 2021, 64, 6037−6058

(17) Comi, G.; Hartung, H. P.; Bakshi, R.; Williams, I. M.; Wiendl, H. Benefit−risk profile of sphingosine-1-phosphate receptor modulators in relapsing and secondary progressive multiple sclerosis. *Drugs* **2017**, *77*, 1755−1768.
(18) Kawasaki, H.; Ozawa, K.; Yamamoto, K. Preparation of pyrazolopyridine compounds and use thereof as remedies for fibrosis. WO 2001098301A1, 2001.
(19) Taylor, R. J. Bicyclic compounds for treatment of inflammatory or allergic conditions and their preparation. WO2008107436A1, 2008.
(20) Naganawa, A.; Kusumi, K.; Otsuki, K.; Sekiguchi, T.; Kakuuchi, A.; Shinozaki, K.; Yamamoto, H.; Nonaka, S. Preparation of phenyl derivatives as S1P2 receptor antagonists. WO 2013047701A1, 2013.
(21) Hla, T.; Jilishitz, I.; Meinke, P.; Stamford, A.; Foley, M.; Sato, A.; Wada, Y.; Fukase, Y.; Asato Kina, A.; Takahagi, H.; Igawa, H.; Polvino, W. J. Pyridinone- and pyridazinone-based compounds and medical uses thereof. WO2019173790A1, 2019.
(22) Satsu, H.; Schaeffer, M. T.; Guerrero, M.; Saldana, A.; Eberhart, C.; Hodder, P.; Cayanan, C.; Schürer, S.; Bhhatarai, B.; Roberts, E.; Rosen, H.; Brown, S. J. A sphingosine 1-phosphate receptor 2 selective allosteric agonist. *Bioorg. Med. Chem.* **2013**, *21*, 5373−5382.
(23) https://www.simulations-plus.com/ (accessed Nov 22, 2020).
(24) Ritchie, T. J.; Macdonald, S. J. F.; Young, R. J.; Pickett, S. D. The impact of aromatic ring count on compound developability: further insights by examining carbo- and hetero-aromatic and -aliphatic ring types. *Drug Discovery Today* **2011**, *16*, 164−171.
(25) Tafazoli, S.; Mashregi, M.; O'Brien, P. J. Role of hydrazine in isoniazid-induced hepatotoxicity in a hepatocyte inflammation model. *Toxicol. Appl. Pharmacol.* **2008**, *229*, 94−101.
(26) (a) Waeber, C.; Salomone, S. Selectivity and specificity of sphingosine-1-phosphate receptor ligands: caveats and critical thinking in characterizing receptor-mediated effects. *Front. Pharmacol.* **2011**, *2*, 1−8. (b) Li, C.; Chi, X. X.; Xie, W.; Strong, J. A.; Zhang, J. M.; Nicol, G. D. Sphingosine 1-phosphate receptor 2 antagonist JTE-013 increases the excitability of sensory neurons independently of the receptor. *J. Neurophysiol.* **2012**, *108*, 1473−1483.
(27) (a) Fang, W. K.; Wang, L.; Corpuz, E.G.; Chow, K.; Im, Wha B. Preparation of condensed pyridine compounds as subtype-selective modulators of sphingosine-1-phosphate-2 (S1P2) receptors. WO2011041287A1, 2011. (b) Swenson, R. E. Preparation of novel N-(pyrazolopyridinylamino) ureas as sphingosine 1-phosphate receptor antagonists. WO2013148460A1, 2013.
(28) Swenson, R. E.; Raju, N.; Estrella-Jimenez, M. E.; Ramalingam, K. Preparation of pyrazolopyridine derivatives for use as S1P2 and SIP5 receptor modulators. WO2011159864A1, 2011.
(29) Verhoest, P. R.; Proulx-Lafrance, C.; Corman, M.; Chenard, L.; Helal, C. J.; Hou, X.; Kleiman, R.; Liu, S.; Marr, E.; Menniti, F. S.; Schmidt, C. J.; Vanase-Frawley, M.; Schmidt, A. W.; Williams, R. D.; Nelson, F. R.; Fonseca, K. R.; Liras, S. Identification of a brain penetrant PDE9A inhibitor utilizing prospective design and chemical enablement as a rapid lead optimization strategy. *J. Med. Chem.* **2009**, *52*, 7946−7949.
(30) Baker, J. G.; Hill, S. J. Multiple GPCR conformations and signalling pathways: implications for antagonist affinity estimates. *Trends Pharmacol. Sci.* **2007**, *28*, 374−381.
(31) Johnson, T. W.; Gallego, R. A.; Edwards, M. P. Lipophilic efficiency as an important metric in drug design. *J. Med. Chem.* **2018**, *61*, 6401−6420. and references therein.
(32) Keane, M. P.; Arenberg, D. A.; Lynch, J. P., III; Whyte, R. I.; Iannettoni, M. D.; Burdick, M. D.; Wilke, C. A.; Morris, S. B.; Glass, M. C.; DiGiovine, B.; Kunkel, S. L.; Strieter, R. M. The CXC chemokines, IL-8 and IP-10, regulate angiogenic activity in idiopathic pulmonary fibrosis. *J. Immunol.* **1997**, *159*, 1437−1443.
(33) O'Sullivan, M. J.; Hirota, N.; Martin, J. G. Sphingosine 1-phosphate (S1P) induced interleukin-8 (IL-8) release is mediated by S1P receptor 2 and nuclear factor κB in BEAS-2B cells. *PLoS One* **2014**, *9*, No. e95566.
(34) Liu, X.; Wright, M.; Hop, C. E. C. A. Rational use of plasma protein and tissue binding data in drug design. *J. Med. Chem.* **2014**, *57*, 8238−8248.
(35) Pennington, L. D.; Moustakas, D. T. The necessary nitrogen atom: a versatile high-impact design element for multiparameter optimization. *J. Med. Chem.* **2017**, *60*, 3552−3579.
(36) Leung, C. S.; Leung, S. S. F.; Tirado-Rives, J.; Jorgensen, W. L. Methyl effects on protein−ligand binding. *J. Med. Chem.* **2012**, *55*, 4489−4500.
(37) Mammoliti, O.; Jansen, K.K.; Palisse, A. E.; Joannesse, C. M. A.-M.; Menet, C. J. M.; Allart, B.; El Bkassiny, S. Preparation of pyridazine derivatives for the prophylaxis and treatment of diseases including fibrosis. WO2017148787A1, 2017.
(38) Moeller, A.; Ask, K.; Warburton, D.; Gauldie, J.; Kolb, M. The bleomycin animal model: a useful tool to investigate treatment options for idiopathic pulmonary fibrosis? *Int. J. Biochem. Cell Biol.* **2008**, *40*, 362−382.
(39) Noble, P. W.; Albera, C.; Bradford, W. Z.; Costabel, U.; Glassberg, M. K.; Kardatzke, D.; King, T. E., Jr.; Lancaster, L.; Sahn, S. A.; Szwarcberg, J.; Valeyre, D.; du Bois, R. M.; CAPACITY Study Group. Pirfenidone in patients with idiopathic pulmonary fibrosis (CAPACITY): two randomised trials. *Lancet* **2011**, *377*, 1760−1769.
(40) Ashcroft, T.; Simpson, J. M.; Timbrell, V. Simple method of estimating severity of pulmonary fibrosis on a numerical scale. *J. Clin. Pathol.* **1988**, *41*, 467−470.
(41) Matsuse, T.; Teramoto, S.; Katayama, H.; Sudo, E.; Ekimoto, H.; Mitsuhashi, H.; Uejima, Y.; Fukuchi, Y.; Ouchi, Y. ICAM-1 mediates lung leukocyte recruitment but not pulmonary fibrosis in a murine model of bleomycin-induced lung injury. *Eur. Respir. J.* **1999**, *13*, 71−77.
(42) Cohen, R.; Graves, C. R.; Nguyen, S. T.; Martin, J. M. L.; Ratner, M. A. The mechanism of aluminum-catalyzed Meerwein−Schmidt−Ponndorf−Verley reduction of carbonyls to alcohols. *J. Am. Chem. Soc.* **2004**, *126*, 14796−14803.
(43) Hayama, T.; Hayashi, K.; Honma, M.; Takahashi, I. Preparation of *N,N′*-biarylurea derivatives as inhibitors of cyclin-dependent kinases (Cdk4 and Cdk6). WO2001007411A1, 2001.
(44) Obach, R. S. The importance of nonspecific binding in in vitro matrices, its impact on enzyme kinetic studies of drug metabolism reactions, and implications for in vitro-in vivo correlations. *Drug Metab. Dispos.* **1996**, *24*, 1047−1049.
(45) Svetnik, V.; Liaw, A.; Tong, C.; Culberson, J. C.; Sheridan, R. P.; Feuston, B. P. Random forest: a classification and regression tool for compound classification and QSAR modeling. *J. Chem. Inf. Comput. Sci.* **2003**, *43*, 1947−1958.

https://doi.org/10.1021/acs.jmedchem.1c00138
J. Med. Chem. 2021, 64, 6037−6058